Journal of Membrane Science & Research

journal homepage: www.msrjournal.com

Review Paper

Loose Nanofiltration Membranes for the Treatment of Textile Wastewater: A Review

Pengrui Jin [1,2], Junfeng Zheng [1], Qieyuan Gao [1], Alicia Kyoungjin An [2], Junyong Zhu [3], Bart Van der Bruggen [1,4,*]

[1] *Department of Chemical Engineering, KU Leuven, Celestijnenlaan 200F, B-3001 Leuven, Belgium*
[2] *School of Energy and Environment, City University of Hong Kong, Tat Chee Avenue, Kowloon, Hong Kong Special Administrative Region*
[3] *School of Chemical Engineering, Zhengzhou University, Zhengzhou 450001, China*
[4] *Faculty of Engineering and the Built Environment, Tshwane University of Technology, Private Bag X680, Pretoria 0001, South Africa*

Article info

Received 2021-09-08
Revised 2022-01-07
Accepted 2022-01-15
Available online 2022-01-15

Keywords

Loose nanofiltration
Textile wastewater
Separation mechanisms
Fabrication methods
Fouling and antifouling

Highlights

- State-of-the-art overview of LNF membranes and its approach to membrane fabrication and modification
- The trend and progress in the development of LNF membranes over the past 3 years
- Fouling and fouling mitigation in the application of LNF membrane
- Future direction in LNF membrane development

Graphical abstract

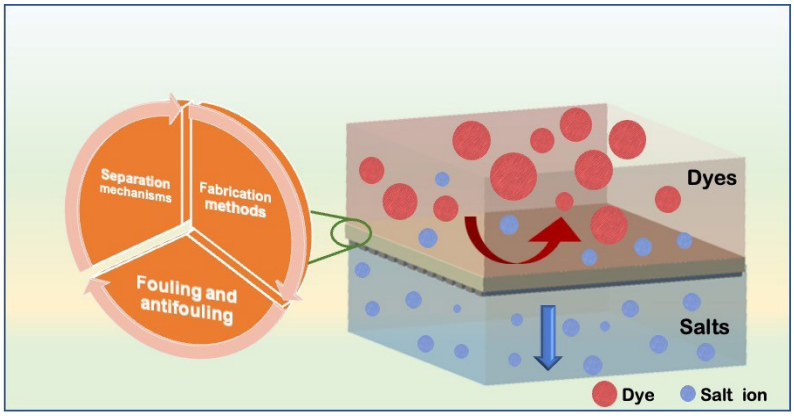

Abstract

Loose nanofiltration (LNF) membrane separation is the fastest-growing textile wastewater treatment technology, due to its tremendous progress in related material and engineering science. Although LNF membranes outperform traditional treatment in the treatment of textile wastewater, the demand for improved selectivity and specificity in membranes separations is growing as we move our focus to the low-energy recovery of valuable compounds from textile wastewater. In this review, we discuss the separation mechanisms for the treatment of textile wastewater, fabrication of LNF membranes, membrane fouling, and control strategies, as well as recent research on LNF membranes. LNF membranes that can achieve high selectivity for dye/salt mixtures, high water permeance, and excellent antifouling performance—as well as the construction mechanisms involved—are highlighted. We further identify practical needs, knowledge gaps, and technological barriers in both material development and structure design for the high selectivity LNF membrane process. Finally, we discuss research priorities in the context of constructing high-performance LNF membranes.

Contents

* Corresponding author: Bart.VanderBruggen@kuleuven.be (B.Van der Bruggen)

DOI: 10.22079/JMSR.2022.538529.1492

1. Introduction

Textile wastewater usually contains a high concentration of salts. In the dyeing process, it is necessary to add inorganic salts, such as up to 2 kg of NaCl or Na_2SO_4 per kilogram of fabric, in the dyeing bath to enhance the adhesion of dyes to the fabric, which is the main source of inorganic salts in the textile wastewater [1-3]. In addition, a by-product of mainly NaCl or Na_2SO_4 can be produced during the dye synthesis process [4]. According to statistics, each ton of traditional dyes can produce at least 15 tons of wastewater [5,6]. The printing and dyeing industry is a major emitter of the textile industry in China, and the average daily discharge of dyeing wastewater alone is as high as 2 million cubic meters [7]. If all of this wastewater is recycled, about 20% of the average daily water consumption of Chinese residents can be saved every year, and about 100, 000 tons of dyes and 10 million tons of inorganic salts can be recycled each year. Therefore, the recycling and treatment of textile wastewater had significant economic and social benefits. However, due to the complicated printing and dyeing process, the composition of the wastewater is complex, which also brings difficulties for its recycling.

The traditional treatment of textile wastewater is divided into three categories: physical (adsorption [8], coagulation [9], and membrane treatment methods [10]), chemical (electrochemical Fenton oxidation [11] and photocatalytic oxidation methods [12]), and biological (aerobic [13], anaerobic [14], and biofilm treatment [15]) methods [16,17]. Comparing various textile wastewater treatment methods, biological methods have the disadvantages of low removal rate for color and chemical oxygen demand (COD), long reaction time, and poor impact resistance. Chemical treatment has several drawbacks, including excessive sludge production, hazardous intermediates, poor applicability, and high operating costs. The adsorption method of physical methods has some problems, such as limited adsorption capacity, difficulties in regenerating the adsorbent, and secondary contamination. The disadvantages of the coagulation method are the need to change the feeding conditions with the change in water quality, the difficulty of practical operation and management, the poor treatment effect of hydrophilic dyes, increased sludge generation, and the difficulty of dehydration. Membrane separation is a high-efficiency separation technology developed in recent decades. Compared with other textile wastewater treatment technologies, it has the advantages of low energy consumption, simple operation, less equipment occupation, and a high degree of automation [18-20]. Simultaneously, membrane separation technology can recycle dyes and inorganic salts in the textile effluent, allowing resource recovery.

Material science of membranes initiated by prof. Yuri Yampolskii has guiding significance for both gas separation and liquid separation [21]. Since the 1960s, liquid separation membrane technology has advanced significantly, and it now has applications in a variety of fields, including the petrochemical industry and organic matter separation. Liquid separation membranes can be classified as ultrafiltration (UF) membranes, nanofiltration (NF) membranes, and reverse osmosis (RO) membranes based on different pore sizes [19]. Compared to UF and RO, NF technology, as a typical membrane separation process with excellent dye rejections, low operating pressure, and low cost is more and more favored by academia and industry [22]. Nanofiltration membranes have pore sizes of 0.5-2 nm, allowing them to extract small molecular weight organics and divalent salts [23]. It is utilized for further treatment and recycling of sewage, textile wastewater treatment, water softening, and heavy metal removal [24]. However, the traditional nanofiltration membranes are unable to separate and recover a mixture of macromolecules/salts, and because the rejection rate of ordinary nanofiltration membranes to inorganic salts and macromolecules is so high, this frequently results in an increase in osmotic pressure during operation, resulting in high energy consumption [25].

In 2004, Van der Bruggen et al. [26] proposed a new concept, a loose nanofiltration membrane, which can effectively separate organic solutes and salts. The LNF membrane is a type of membrane with nanofiltration and ultrafiltration boundary pore sizes that can fully separate organic matter (in the range of 500~2000 Da)/salt mixtures. As a result, the LNF membrane can be used to remove small organic macromolecules that are too small to be captured by ultrafiltration while allowing salt ions to flow through. The water permeance of the LNF membrane, on the other hand, is much larger than that of the tight nanofiltration membrane, which can filter faster at lower pressure [1]. For example, Liang et al. [27] tested LNF membranes for the treatments of dyes (acid, basic and reactive dyes) wastewater in a series of experiments. Using lab-scale tests, they confirmed that LNF could be integrated with coagulation/flocculation processes to provide efficient textile wastewater treatment [27]. Inspired by this, they further scaled up this technology to a pilot scale for the treatment of actual textile wastewater [28]. Thong et al. [29] produced LNF hollow fiber membranes for textile wastewater treatment with high rejection (94.9%) for indigo carmine via using a single-step spinning process. Compared to flat-sheet LNF membranes, LNF membranes in the hollow fiber configuration can provide high packing density and self-supporting properties. Currently, some commercial NF membranes have been applied in the treatment of textile wastewater; the basic parameters of the membranes are shown in Table 1. Although these commercial NF membranes are effective at retaining dye molecules, the pure water permeance of the membranes still needs to be improved, and the salt passage performance of the membranes also has considerable room for improvement. At the same time, LNF membranes with special capabilities, such as antifouling, antibacterial, and photocatalytic ability, need to be developed.

Currently, encouraging demonstrations using LNF membranes have attracted increasing attention for resource recovery especially for selective separation of dyes and inorganic salts, but so far, no comprehensive review has focused specifically on this rapidly growing field. This review focuses on LNF membranes with emphasis on textile wastewater treatment. Particularly the LNF membranes preparation, fouling, and fouling mitigation strategies are emphasized. Current research challenges and the possible focus of further research on LNF membranes are proposed.

2. Separation mechanism of LNF membranes

The mass transfer and selective separation mechanism of LNF membranes has been a key research issue. LNF membranes are generally charged separation membranes with nano-scale microporous structures. The pore size of an LNF membrane is about 1.5-2 nm, and the corresponding molecular weight cut-off is about 500-2000 Da [22,37,38]. Currently, there are not enough studies on the separation mechanism of LNF membranes, but there have been a lot of studies on the separation mechanism of NF membranes, which can serve as motivation for LNF separation research. Therefore, a brief overview of NF mechanism is given here. There are usually a lot of negative charges on the surface of commercial NF membranes. Hence, the synergy of the tree factors of size sieving, Donnan effect and dielectric effect is generally considered to be the separation mechanism of NF membranes, as shown in Figure 1 [39].

Size sieving can be the basis to describe the transmembrane mass transfer behavior of neutral solutes across NF membranes [40]. The NF membrane is effective at rejecting neutral solutes with a size larger than its pore size. If the neutral solutes are to enter the membrane channels, the membrane materials must be distorted to increase the pore size, or the neutral particles must be deformed to reduce the solute size, but both need to overcome huge energy barriers [18,41,42]. Even when the size of neutral solutes is below the pore size of the membrane, only part of neutral solutes penetrates the channels of such NF membrane. The pore size of an NF membrane can be correlated with its separation performance for neutral solutes [18]. Therefore, the pore size and pore size distribution can be indirectly determined by measuring the rejection of a sequence of neutral organic molecules of various sizes in an aqueous solution. Although the size sieving effect can explain the transmembrane mass transfer behavior of neutral particles in NF membranes, it is not fully used in electrolyte solutions, especially for electrolytes with a size below the pore size of NF membranes. Considering that NF membranes contain ionizable functional groups when NF membranes are employed for electrolyte solution separation, there will be a certain electrostatic interaction between charged functional groups and ions on its surface and its pore channels; the charged functional groups repel their common ions and attract their counter ions, thereby preventing or boosting the distribution of ions in the pores of NF membranes [43,44]. Therefore, the charge of an NF membrane in an aqueous solution is one of the most significant properties to determine its separation performance. The chemical structure of an NF membrane determines its charge in an aqueous solution, which is also influenced by the pH of the solution. If amphoteric functional groups, such as amino and carboxyl groups, are present in the chemical structure of the NF membrane, the NF membrane will have an isoelectric point, that is, the pH value at which the NF membrane turns neutral in an aqueous solution. Carboxyl ionization takes over when the pH value is above the isoelectric point, and the NF membrane becomes negatively charged in the aqueous solution; while when the pH value is below the isoelectric point, carboxyl ionization is hindered, amino protonation is dominating, and the overall charge of the NF membrane is positive. The surface charge properties of NF membrane in an aqueous solution can be characterized by measuring the zeta potential at different pH values. The dielectric repulsion effect is due to the difference between the dielectric constant of water and that of the membrane material, which results in the tendency of all ions to be rejected by the NF membrane [45,46].

Table 1
Commercial NF and LNF membranes.

Supplier	Membranes (MWCO)	Operation pressure	Permeance (LMH bar^{-1})	Dyes rejection	Salts rejection	Ref.
GE Osmonics	DK (~150-300 Da)		10		$MgSO_4$ =96%	[30]
Ultura	Sepro NF 2A (529 Da)	6 bar	10.5	Direct red 80=99.98% Direct red 23=99.95% Congo red=99.96%	NaCl (20g L^{-1})=30%	[1, 31]
Ultura	Sepro NF 6 (847 Da)	6 bar	13.7	Direct red 80=99.95% Direct red 23=99.76% Congo red=99.93%	NaCl=10%	[1, 31]
State Oceanic Administration, Hangzhou, China	CA	10 bar	8.1	Reactive orange 12>99% Reactive red 24>99% Reactive black 5>99% Reactive blue 74>99% Reactive blue 13>99%	Na_2SO_4 (2g L^{-1})=~40% NaCl (2g L^{-1})=~10%	[32]
Osmonics Desal	DK	30 bar		Reactive black 5=96%	Salt =21.1%	[33]
	DK 2540F (~300 Da)	8-12 bar		Direct dyes and reactive dyes=100%	Salts =47-52%	[34]
GE Osmonics	DS5 DK (150-300 Da)	8-30 bar	6.6	Reactive black 5>99% Reactive orange 16>99% Reactive blue 19>99%		[35]
Koch	TFC-SR2	5 bar	~5	Reactive black 5=~98%	NaCl (20g L^{-1}) <14%	[36]

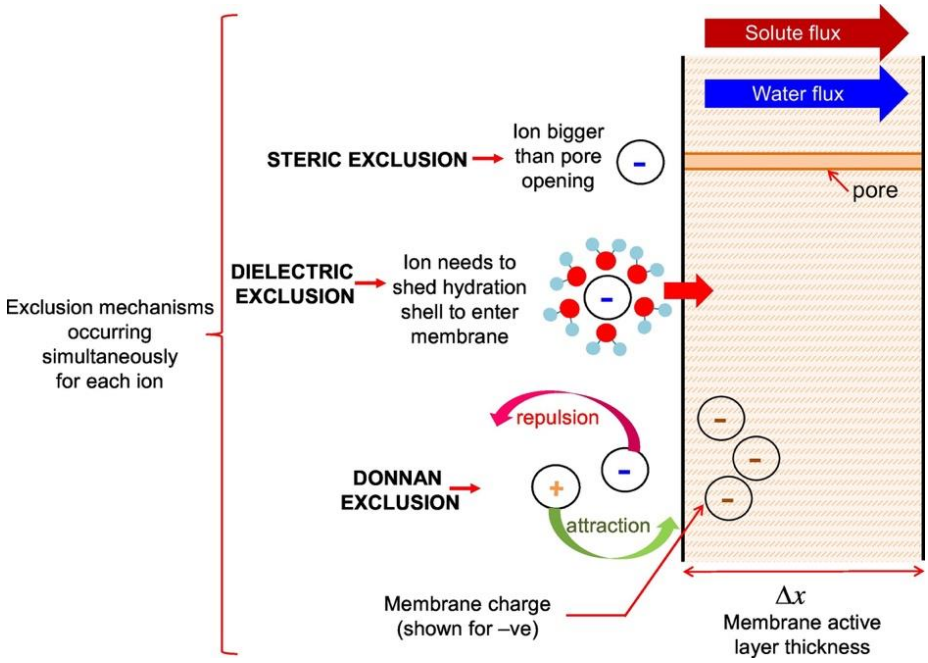

Fig. 1. Schematic representation of solute exclusion mechanisms in nanofiltration [39].

The separation principle of LNF membranes for dye/salt mixtures is different from that of an NF membrane. For an LNF membrane, the sieving effect is dominant, and large molecules are trapped on the membrane surface. Guo et al. [47] performed a preliminary study on the effect of trace pollutants in glycerol/water during LNF membranes preparation on membrane pore size distribution and separation performance, which has reference significance for the study of LNF separation mechanisms. In addition to the size sieving effect, electrostatic repulsion also affects the separation process of LNF membranes. Some anionic dyes, such as reactive dyes (reactive blue 2, reactive black) and direct dyes (Congo red), have a higher actual rejection than theoretical calculations. This is due to the aggregation of dye molecules resulting in an increase in size; whereas the negatively charged dye molecules aggregate and create stronger electrostatic repulsion, resulting in higher rejection rates.

3. Fabrication of LNF membranes

There are several key approaches to fabricating LNF membranes, which are determined by the membrane fabrication method and membrane material. In this review, a brief overview of these important methods is given: interfacial polymerization, phase inversion, deposition, vacuum filtration, graft polymerization, self-assembly, and others. All of these technologies are designed to develop LNF membranes with higher water permeance, better selectivity for dye/salt mixes, and fouling resistance.

3.1. Interfacial polymerization (IP)

Interfacial polymerization (IP) is the most extensively utilized NF membrane fabrication process in the world. The IP method is based on Morgan's principle of phase-interface polymerization, which enables two reactants in incompatible phases to undergo IP on the surface of the supporting membrane, and then be combined with an ultrathin selective layer, which determines the final performance of the NF membrane [48,49]. As shown in Table 2, the IP method can also be used to prepare LNF membranes for dye/salt separation. In recent years, to improve the separation performance of LNF membranes, researchers have tried to find new monomers, nanoparticle doping, post-treatment, and other strategies to improve the IP process.

As shown in Figure 2, monomers with lower reactivity and a larger size can result in a selective layer of LNF membrane with larger pore size and lower crosslinking degree, which structure is beneficial for separating dye/salt mixtures [50]. As shown in Table 2, hydroxyl-containing monomers are commonly employed as aqueous phase monomers to prepare polyester LNF membranes due to their large size and low reactivity. For example, Jin *et al.* [51] used erythritol to fabricate polyester LNF membrane via IP with excellent antifouling performance. The prepared polyester selective layer by erythritol has a loose structure and negative surface charge, showing high water permeance, high rejection of dyes (>95%), and high transmission of salts (>90%). Besides, many other hydroxyl-containing monomers, such as cyclodextrin [52-54], and sugars [50], have also been successfully applied in the preparation of LNF membranes for the separation of dyes and salts. The aforementioned LNF membrane design principles are not just applicable for polyester LNF membranes, but also polyamide LNF membranes. For example, Kang et al. [55] obtained a negatively charged polyamide LNF membrane with a loose inner structure using *L*-lysine as an aqueous phase monomer. It was reported that the *L*-lysine with large size and electriferous groups could tailor the LNF membrane separation performance by loosening the inner structure and enhancing the Donnan effect, resulting in a polyamide LNF membrane with high dye rejection (>99%) and high salt permeability (>97.5%).

Aside from the use of new monomers with large size or low reactivity, the addition of nanoparticles and additives can also be employed to control the pore structure of traditional piperazine-trimesoylchloride (PIP-TMC) NF membranes. Some researchers attempted to introduce nanomaterials, such as carbon quantum dots (CQD) [56-58], graphene quantum dots (GQD) [54,59,60], TiO_2 [61], into the aqueous or organic phase to control the IP process, build transport channels, or produce a loose polyamide structure for molecular sieving. As shown in Figure 3, Sun et al. [56] designed a novel LNF membrane by incorporating CQDs-NH_2 into the aqueous monomer phase. The resultant membrane permeance increased from 6.2 to 38.4 LMH bar^{-1} with high rejection of dyes and low rejection of salts. Efforts were also made to prepare LNF membranes via adding additives in the aqueous monomers phase. These additives can increase the length of monomer in the aqueous phase [62], synthesize pH-responsive LNF membranes with adjustable permeability and selectivity [63], or make the resultant membrane lose its structure after post-treatment [64]. Li et al. [62] proved that tannic acid mixed with PIP can enlarge the pore size of the polyamide selective layer to achieve high water permeance with excellent dye/salt separation ability (Figure 4a). He et al. [63] prepared a pH-responsive LNF membrane by IP with a mixture of PIP and chitosan as the aqueous phase and TMC as the organic phase (Figure 4b). The results showed that the water flux of the synthesized membrane increased from 49.6 to 128.8 LMH bar^{-1} by increasing the pH from 8 to 12 and the membrane pore size changed somewhat. Furthermore, the resultant LNF membrane showed precise separation performance for dye/salt or dye/dye mixtures at pH 12. Another facile and effective approach to modulate the structure and surface properties of the selective layer of NF membranes is post-treatment, such as alkaline post-etching. Luo et al. [64] prepared a polyester-polyamide composite NF membrane by the IP process with PIP and tannic acid as the aqueous phase monomers and TMC as the organic monomer, and then proposed an alkaline treatment to etch the polyester structure to obtain LNF membranes (Figure 4c).

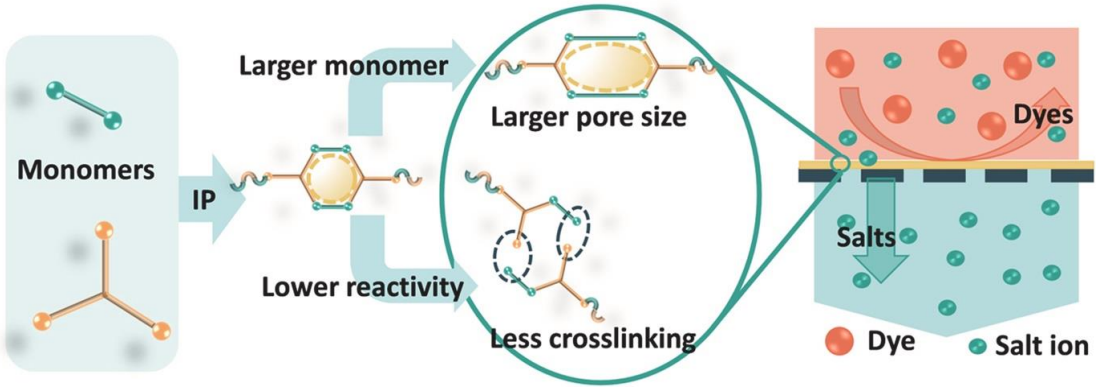

Fig. 2. Strategy and mechanisms to enlarge the pore size of the LNF membrane via IP [50].

In recent years, numerous innovative membrane production methods (electrospray IP [65], integration of phase inversion and IP [66], combining blending with IP [67]) and materials (covalent organic frameworks (COFs) [68-70]) based on the IP process have arisen for the preparation of high-performance LNF membrane. Kim et al. [65] fabricated an LNF membrane with excellent performance for dye wastewater treatment using electrospray IP with PIP and TMC as building monomers. The resulting LNF membranes demonstrated high permeance and selectivity for dye/salt mixtures separations, compared to regular PIP-TMC NF membranes. Chen et al. [71] combinate the advantages of phase inversion and interfacial polymerization to prepare a polyamide/poly(vinylidene fluoride) composite hollow fiber membrane during the fiber spinning process (Figure 5a). The created membrane with an outer-selective layer showed high dyes rejection (>98%), low salts rejection (NaCl 6.2%), and remarkable water permeance of 10.2 LMH bar^{-1}. To create a unique LNF membrane, Qin et al. [67] combine blending with IP, by incorporating styrene-maleic anhydride (SMA) into PVDF to supply numerous carboxyl groups, then PEI and triethanolamine were co-deposited on the membrane surface by IP reaction and hydrogen bonding. The resultant membrane showed an excellent fractionation ability for dye/salt mixtures with high water permeance of up to 251.6 LMH bar^{-1}. Recently, interest in COFs for the preparation of LNF membranes has grown, due to their unique ordered porous structures, which could be employed for precise dye/salt or dye/dye separation with high water permeance [68-70]. For example, Zhang et al. [68] adopted an in-situ IP of COFs selective layer upon polysulfone substrate to form COFs-based LNF membranes, as shown in Figure 5b. The as-prepared membranes exhibited a Congo red rejection above 99% and excellent water permeance of 62.2 LMH bar^{-1}.

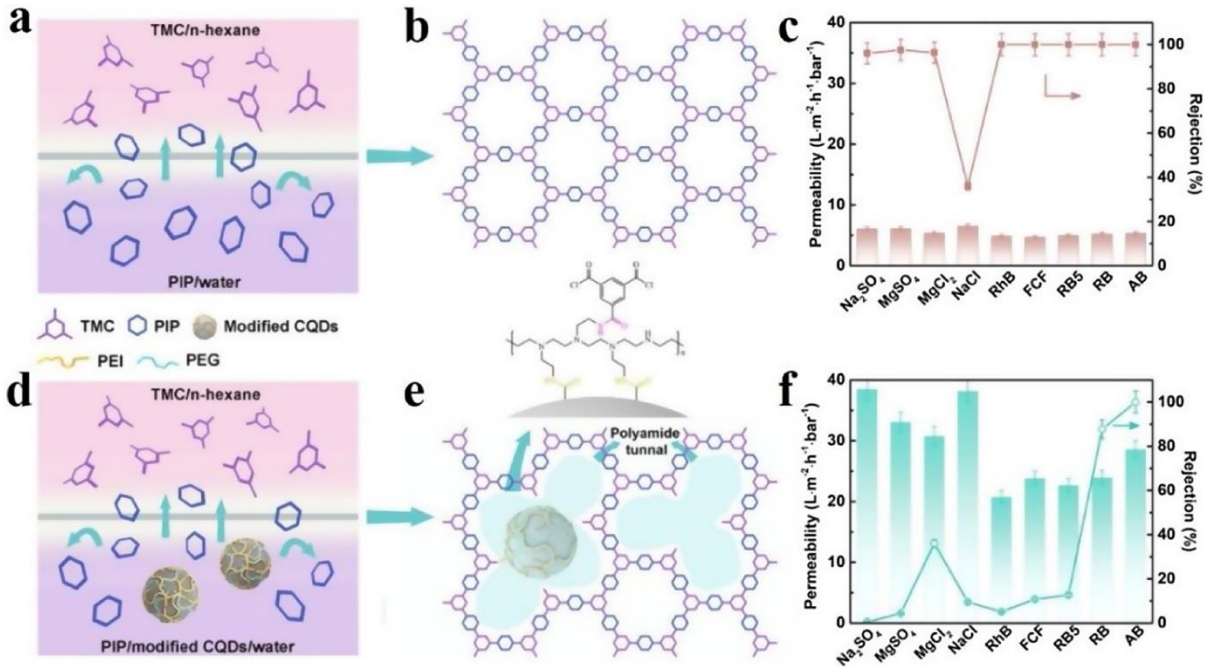

Fig. 3. The possible schematics of LNF membrane structures and performances formation in different IP processes [56].

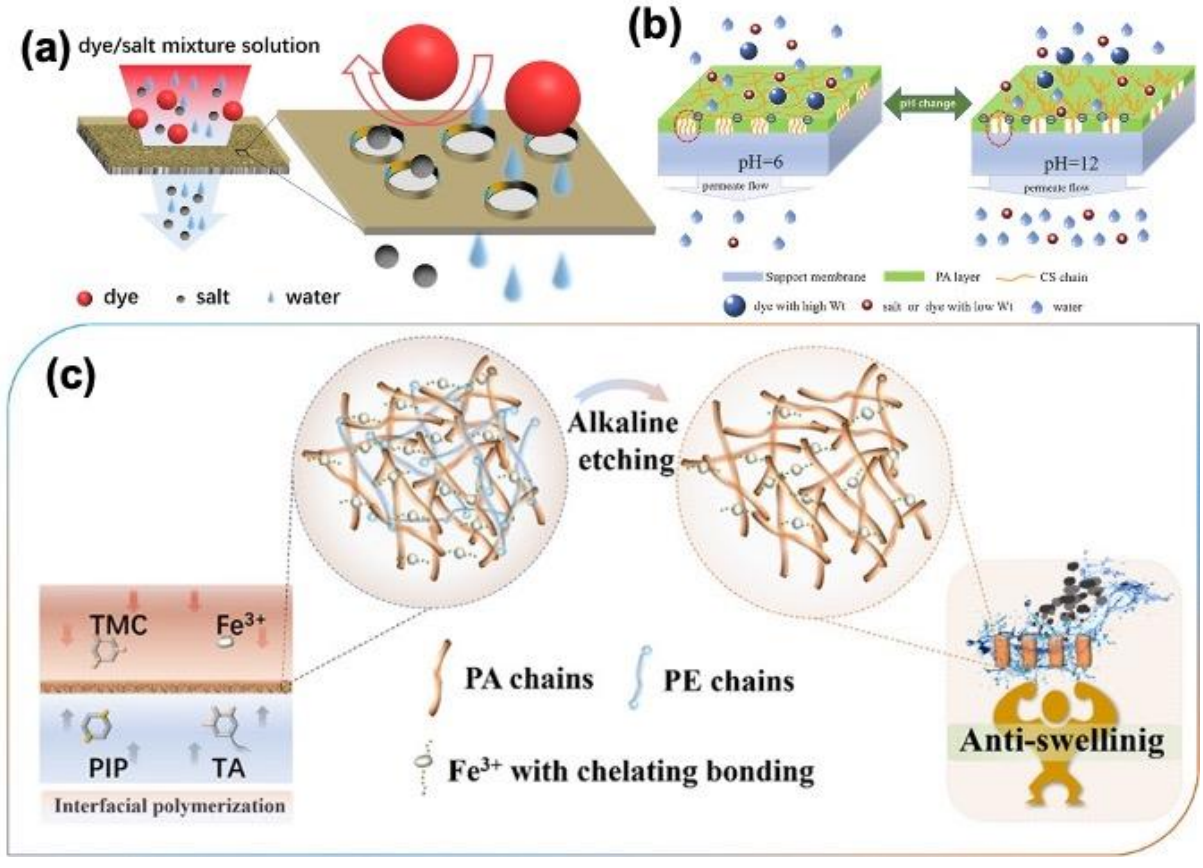

Fig. 4. (a) Tannic acid assisted IP-based LNF membrane [62], (b) pH-responsive LNF membrane containing chitosan [63], (c) LNF membrane prepared by 'selective-etching-induced reinforcing' strategy [64].

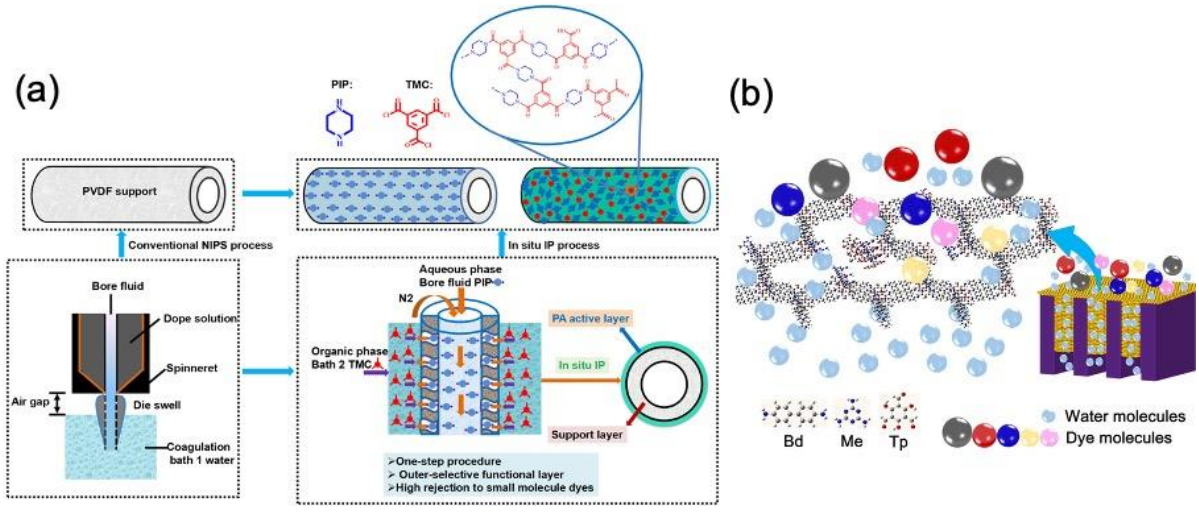

Fig. 5. (a) In-situ synthesis hollow fiber LNF membranes [71], (b) COF-based LNF membrane prepared via IP [68].

Table 2
Properties of the LNF membranes prepared by IP method with new monomers or co-reactants.

Monomers (Water-organic)	Operation pressure	MWCO/pore size	Permeance (LMH bar^{-1})	Dyes rejection	Salts rejection	Ref.
ME-TMC	4 bar	-	53.2	Congo red=99.6% Direct red 23=95.2% Reactive blue 2=99.6%	Na_2SO_4 (1g L^{-1})=11% NaCl (1g L^{-1})=5.6%	[51]
Hydroxyl-containing monomers-TMC	2 bar	1070 Da	115.9	Congo red=99.4% Direct red 23=98.3% Reactive blue 2=92.1%	Na_2SO_4 (1g L^{-1})=1.3% $MgSO_4$ (1g L^{-1})=0.4% $MgCl_2$ (1g L^{-1})=0% NaCl (1g L^{-1})=1.1%	[50]
PIP/TA-TMC/$Fe(acac)_3$	20 bar		17	Color removal efficiency=95%		[64]
Melamine/ZnTCPP +TMC	2 bar	3376 Da	63.2	Congo red=99.9% Direct red 23=98.5% Methyl blue=96.7%	Na_2SO_4 (1g L^{-1})=10.1% NaCl (1g L^{-1})=1.6%	[72]
PIP/CQDs-NH2+TMC	6 bar	-	38.4	Alcian blue=100% Rose Bengal=89% Reactive black 5=18% Fast green=17%	Na_2SO_4 (1g L^{-1})=1% $MgSO_4$ (1g L^{-1})=3% $MgCl_2$ (1g L^{-1})=18% NaCl (1g L^{-1})=4%	[56]
GQDs/PIP/BP+ TMC	6 bar	1107 Da, 1.07 nm	56	all selected dyes>99.8%	Salts (1g L^{-1})<8.8%	[59]
β-CD/TMC-MWCNTs	1 bar	590 Da	179.3	Brilliant green=97.4% Congo red=96.4%	Na_2SO_4 (1g L^{-1})=98.4% $MgSO_4$=26% $MgCl_2$=30% NaCl=20%	[52]
β-CD/TMC	2 bar	-	103.9	Congo red=100% Rose Bengal=99.1	NaCl (2g L^{-1})=8.5%	[53]
GQDs-TMC-PABA	0.5 bar		128.1	Evans blue=99.5%	Na_2SO_4 (1g L^{-1})=12.6% NaCl (1g L^{-1})=3.1%	[60]
PA/TpPa-12/PAN	6 bar	280 Da	21	Congo red=100%	NaCl (2g L^{-1})=20%	[73]
CQDs/MPD/MTH-TMC	8 bar	0.46 nm	4.31	Small sized organics=97%		[57]
PIP/chitosan+TMC	5 bar	pH2, 438 Da, 0.54 nm	128.7	Congo red>99%	Na_2SO_4 (1g L^{-1})=9.7%	[63]

		pH6, 543 Da, 0.56 nm pH12, 8.64 nm		Methyl blue>99% Coomassie brilliant blue G250>99%		
PEI/QGO/QCQDs+ TMC	4 bar	0.433 nm	23.8	Cationic trimethoprim=99.7% Atenolol=99.5% Rhodamine B=98.9% Methylene blue=98.4%	$MgCl_2$(0.5g L^{-1})=95.7%	[58]
PIP-TMC/UiO-66-NH2	2 bar	-	36.7	Methyl orange=92.2% Sunset yellow=95.9% Congo red=99.6%	NaCl(1g L^{-1})=9.7%	[74]
HFM-PIP/TMC	2 bar	4200 Da, 0.72 nm	10.2	Congo red=100% Eriochrome black T=100% Rhodamine B=99.9% Methyl blue=99.9	NaCl(1g L^{-1})=6.2%	[71]
SPEI+TMC	6 bar	-	41.1	Victoria blue b>97% Congo red>97% Methyl blue>97% Reactive red 120>97%	Na_2SO_4(1g L^{-1})=8.4% NaCl(1g L^{-1})=3.2%	[75]
Electrospray IP (PIP/TMC)	5 bar	1800 Da	20.2	Congo red=99.6%	NaCl(1g L^{-1})=6.3%	[65]
Polyester amine-TMC	4 bar	490 Da	16.6	Methyl blue=95.4%	NaCl(1g L^{-1})=16.4%	[76]
TA/PIP-TMC		1370 Da	32.6	Congo red=99.4% Rose Bengal=99.2%	Na_2SO_4(2g L^{-1})=9.4% NaCl(2g L^{-1})=2.3%	[62]
β-CD/GQDs-TMC	1 bar	2.3 nm	280	Eriochrome Black T=97.1% Congo red=96.4% Alican blue=90.9% Methyl blue=86.2%	Na_2SO_4(1g L^{-1})<20%	[54]
L-lysine+TMC	6 bar	1150 Da	38.5	Naphthol green B=99.2%	NaCl(2g L^{-1})=2.7%	[55]
Tp-Bd-Me/PSf	2 bar	2.2 nm	62.2	Congo red =99%		[68]
PANI-TpPa/HPAN		1.8 nm	85.2	Congo red =99.4% Acid fuchsin=81%		[69]
TiO_2-PIP-TMC	2 bar	-	65	Congo red =99.4% Alican blue=96% Orange GII=85%	Na_2SO_4(1g L^{-1})=17%	[61]
SMA+PEI+TEA	2 bar	1350 Da	256.1	Congo red=99.9% Methyl blue=96.7% Acid fuchsin=96.1%	$MgSO_4$(1g L^{-1})=1.2% $MgCl_2$(1g L^{-1})=4.5% NaCl(1g L^{-1})=1.7%	[67]
TFPB+EDA	5 bar	800 Da	49.5	Brilliant blue-R 825=100%	Salts(2g L^{-1})<10%	[70]

3.2. Nonsolvent induced phase separation (NIPS)

The phase inversion method was first used by Loeb and Sourirajan in the 1960s [77]. This technology has become the most extensively used method for manufacturing asymmetric polymer membranes because of its low cost and high reproducibility. As shown in Figure 6, the polymer casting solution is immersed in a non-solvent bath, and the phase inversion occurs under the double diffusion of the solvent and non-solvent; the polymer precipitates at the solvent and non-solvent interface, forming a dense layer with selective separation and a porous layer with mechanical support. Phase inversion is a typical approach for creating microfiltration and ultrafiltration membranes; it is not easy to obtain NF membranes with high salts rejection. Phase inversion, on the other hand, is an excellent choice for LNF membranes with high salt permeability and high dyes rejection. Table 3 summarizes recent research findings on high-performance LNF membranes manufactured via phase inversion.

The key to preparing LNF membranes using the phase inversion method is to control the membrane hydrophilicity and pore size. The membrane pore size is mainly affected by the composition of the casting solution and the phase separation process. The unique structure and features of nanoparticles can alter the phase inversion process of the polymer casting solution, allowing the final membrane structure, hydrophilicity, and pore size to be adjusted, hence improving the separation performance of the LNF membrane. Zhang et al. [79] fabricated mixed-matrix membranes comprising charged nanomaterial SiO_2-SBMA as the fillers and polyvinylpyrrolidone (PVP) and PES as the polymeric matrix for textile wastewater treatment via phase inversion. The SiO_2-SBMA was prepared by nano SiO_2 and 2-methacryloyloxy ethyl dimethyl (3-sulfopropyl)-ammonium hydroxide sulfobetaine methacrylate

(SBMA). The SiO_2-PSBMA/PES LNF membrane showed effective dye/salts separation with high water flux. Tavangar et al. [80] developed and demonstrated highly hydrophilic and porous CeO_2-PES LNF membranes by incorporating CeO_2 into a PES matrix for dye solution purification and resource recovery. This membrane showed water permeance of 26.2 $Lm^{-2}h^{-1}bar^{-1}$, which is 4 times higher than that of the bare PES polymer membrane. Zhang et al. [81] incorporated both PANI and GO with high hydrophilic nature into a PVDF casting solution to prepare an LNF membrane via phase inversion. The resultant PVDF-PANI-GO LNF membrane with improved antifouling properties showed a maximum of 98% of dye rejection at super low operation pressure (1 bar) (Figure 7).

Hydrophilic inorganic nanoparticles as additives are a straightforward and effective way to control the structure and hydrophilic characteristics of LNF membranes by phase inversion, but they have some drawbacks. Because the blending modification is a physical method, the nanoparticles may be gradually removed from the polymer matrix during the use of the membrane, causing the modification effect to deteriorate. One option to tackle this problem is to employ organic additives that are more compatible with the polymer as blending modification alternatives during the phase inversion process [82-84]. Padaki et al. [82] developed a carboxylate poly(ionic liquid) (PIL)/PSf blend selective LNF membrane with hydrophilic nanochannels, as shown in Figure 8. The blended membrane has exceptional stability in an aqueous solution due to the chemical interaction between PIL and PSf. Furthermore, the PIL/PSf LNF membrane achieves high water permeance of up to 100 LMH bar^{-1} while maintaining a high dye rejection (>98%). In recent years, additives to fine-tune morphology as well as hydrophilicity were explored for LNF membrane fabrication. For example, Li et al. [83] added dicarboxylic acids and aliphatic alcohols into a PES casting solution to prepare LNF membranes. Low-content organic additives have been shown to successfully modify the membrane morphology and hydrophilicity, resulting in LNF properties. The phase inversion approach can also be employed to prepare hollow fiber LNF membranes, as shown in Figure 9 [29, 85]. Hollow fiber LNF membranes provide superior self-supporting properties, good antifouling properties, quick backwashing, a simple membrane module, and a high filling density of membrane module, as compared to flat membranes [85,86].

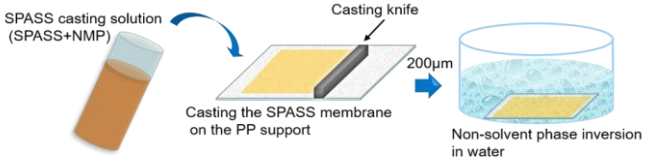

Fig. 6. Schematic presentation of the fabrication of PATS/SS membrane and oxidized PATS/SS membrane [78].

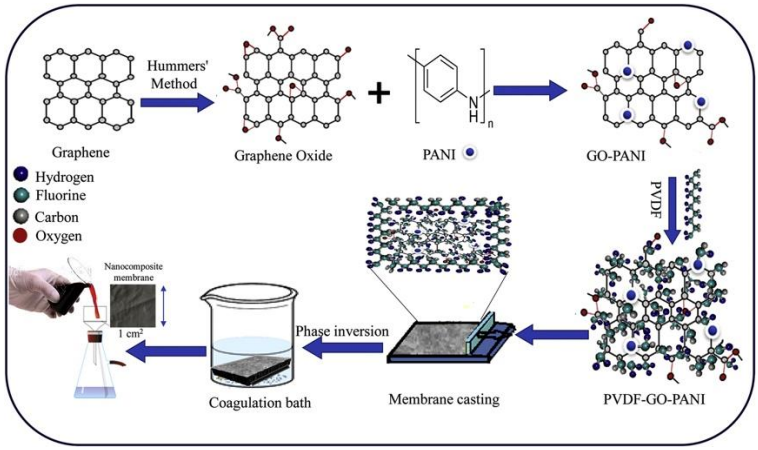

Fig. 7. Schematic representation of membrane fabrication through phase inversion method [81].

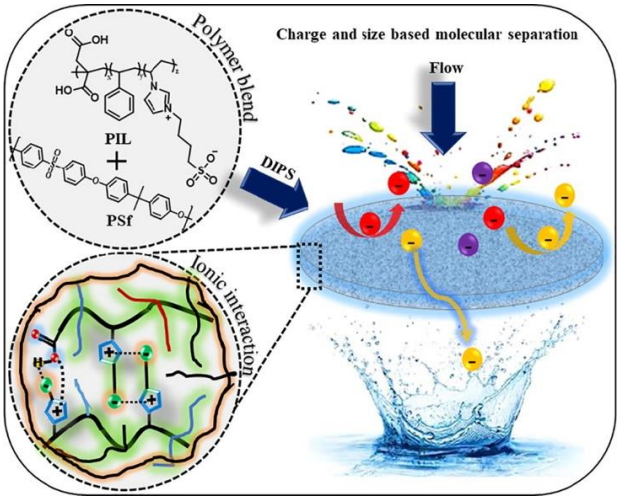

Fig. 8. Schematic representation of PIL/PSf based membrane [82].

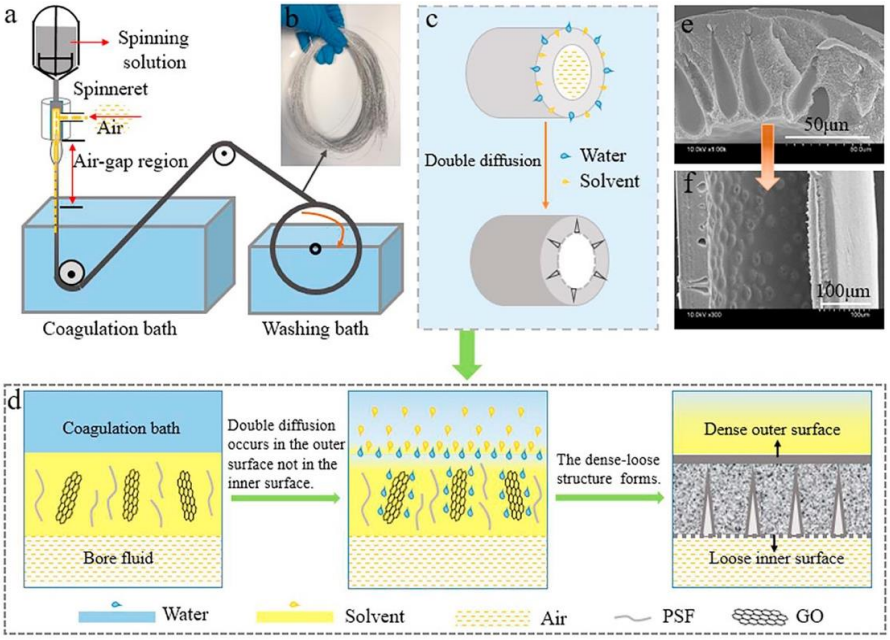

Fig. 9. Preparation process and structure of hollow fiber LNF membrane [85].

Table 3
Properties of the LNF membranes prepared by NIPS process.

Membrane materials	Operation pressure	MWCO/pore size	Permeance (LMH bar^{-1})	Dyes rejection	Salts rejection	Ref.
PES/C5/C9	2 bar		~200	Congo red=97%	Na_2SO_4=3~12%	[83]
PSF-b-PEG	3 bar	1.3 nm	49.3	Congo red>98%	Na_2SO_4(2g L^{-1})=0%	[87]
PES/SPSF	2 bar	7250 Da, 1.8 nm	72.2	Methyl orange=69.4% Acid blue 25=92.6% Evans blue=100%	Na_2SO_4(1g L^{-1})=20%	[88]
CeO_2-PES	5 bar	-	26.24	Direct red 23=99.5% Congo red=99.4% Direct red 243=99.8%	Na_2SO_4(1g L^{-1})=3.3% $MgSO_4$(1g L^{-1})=4.1% $MgCl_2$(1g L^{-1})=1.8% NaCl(1g L^{-1})=1.2%	[80]
SPEI+TMC	6 bar	-	41.1	Victoria blue b>97% Congo red>97% Methyl blue>97% Reactive red 120>97%	Na_2SO_4(1g L^{-1})=8.4% NaCl(1g L^{-1})=3.2%	[75]
SiO_2-PSBMA/PES	4 bar	-	32.3	Reactive black 5=97.9% Reactive green 19=99%	Na_2SO_4=11.4%	[79]
PES/SMA-PEI	2 bar	-	23	Congo red=99.4%	NaCl(1g L^{-1})=2.5%	[89]
PANI-GO+PVDF	1 bar	-	454	Methyl orange=95% Allura red=94%		[81]
SPSf+PES+DMAc	1 bar	-	110.4	Evans blue=99% Coomassie brilliant blue=99.9% Congo red=99.2% Acid fuchsine=90.1%	Na_2SO_4(5-40g L^{-1})<5%	[84]
PSF/GO	2 bar	2.5 nm	36.9-47.7	Congo red=99.9%	NaCl(1g L^{-1})<5%	[85]
PEI-Torlon&sPPSU	1 bar	-	80	Various dyes=95.5-99.9%	Na_2SO_4(2g L^{-1})<10%	[86]
PIL+PSf	2 bar	1.5 nm	100	Eriochrome black t=99% Congo red=99.9%	Methyl orange<3%	[82]

3.3. Bio-inspired deposition

Mussels produce an adhesive substance that allows them to adhere to solid objects in the ocean. Bio-inspired deposition, e.g., catechol-amine chemistry dopamine self-polymerization, is a method for preparing composite NF membranes, which is developed based on this mussel adhesion mechanism. The polydopamine (PDA) precipitation procedure is not only suited for the modification of various materials, but also necessitates gentle precipitation conditions, which can be accomplished at room temperature and in an open atmosphere. As shown in Table 4, inspired by the preparation method of mussel-inspired deposition, various strategies have been developed to prepare high-performance LNF membranes by addressing the inherent shortcomings of PDA deposition.

The traditional PDA deposition procedure takes a long time, usually more than 12 hours, resulting in a thick coating with high mass transfer resistance; however, due to the dopamine self-polymerization, a short coating period would result in many flaws and poor separation performance. Therefore, adding extra oxidants (e.g., $CuSO_4/H_2O_2$ [90], $FeCl_3/H_2O_2$ [91], and ammonium persulfate [92]) in the dopamine solution system to speed up the self-polymerization of dopamine and the production of the selective layer of the nanofiltration membrane can improve the quality of the resultant membrane. Zhang et al. [90] used $CuSO_4/H_2O_2$ as a trigger to achieve rapid PDA deposition on diverse substrates, which served as a benchmark for further research. Following that, Zhu et al. [93] employed $CuSO_4/H_2O_2$ as an initiator to swiftly deposit the PDA layer on the PAN substrate, resulting in the LNF membrane that can be made in less than an hour (Figure 10). The prepared CuNP/PDA-PAN LNF membrane can achieve a good dye/salt separation while maintaining long-term operation stability, antifouling, and antibacterial properties.

Furthermore, the expensive cost of dopamine restricts its industrial application. Other low-cost polyphenols, such as tannic acid (TA) [94-96], gallic acid (GA) [97], epigallocatechin gallate (EGCg) [98], and catechol, can react with polyamino compounds in a dopamine-like fashion, and their bionic co-coating system has received extensive attention. As shown in Figure 11, Li et al. [95] reported a green rapid coating process by adding PEI and TA to form the co-deposition solution. The prepared PEI-TA/PES LNF membrane with desirable permeability (40.6 LMH bar^{-1}) showed a high rejection of dyes and high permeation of salts. Wang et al. [99] prepared a separation layer with a loose structure by depositing catechol and PEI on the PES substrate with $CuSO_4/H_2O_2$ as a trigger. Due to the presence of catechol groups and residual copper ions, the obtained membrane maintains excellent LNF performance and has long-term antibacterial stability, which is beneficial to slow down the fouling formation during the long-term operation.

On the other hand, polyphenols such as dopamine, TA, GA can not only react with amino substances but also interact with two-dimensional materials to achieve the purpose of high permeability [94,100]. Kang et al. [94] used functionalization agents of TA/Ni^{2+} to expand the d-spacing of GO nanosheets by bio-inspired strategy. The obtained membrane showed high permeance (71.7 LMH bar^{-1}) and high salt permeance without sacrificing its high dye rejection. In recent years, zwitterionic polymers have attracted a lot of interest, due to their strong hydrophilic properties, which can endow membranes with antifouling capabilities [100,101]. As shown in Figure 12, Zhang et al. [100] combined the high flux provided by MoS_2 with the antifouling ability provided by zwitterionic polymers through vacuum filtration and co-deposition to prepare LNF membranes with excellent performance.

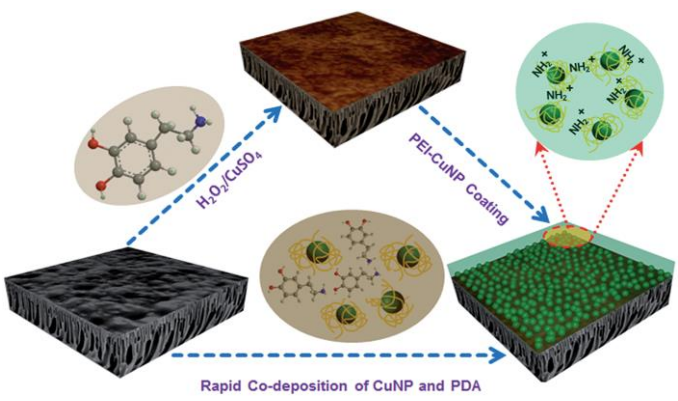

Fig. 10. LNF membranes were prepared via fast bioinspired deposition [93].

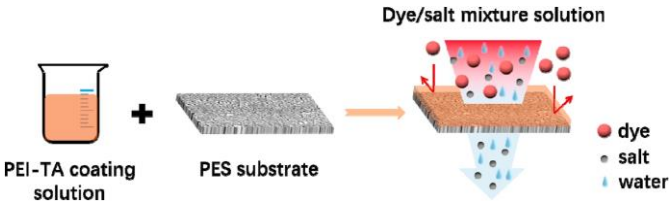

Fig. 11. Green rapid coating process and dye/salt separation of PEI-TA/PES membrane [95].

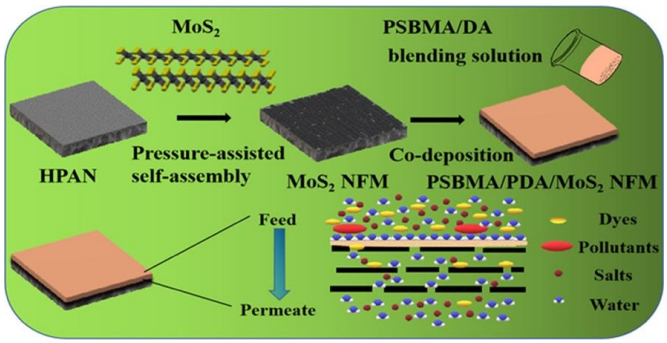

Fig. 12. High-flux Zwitterion-Modified MoS_2 Membranes [100].

3.4. Vacuum filtration

The difference between ambient pressure and the vacuum causes vacuum filtration, which uses the pressure gradient as the driving force, as shown in Figure 13. This technology is inexpensive and simple to scale up. The structure of LNF membranes with a two-dimensional (2D) selective layer by simple and easy vacuum filtration shows a unique pattern different from a traditional polymer membrane. The most common method is vacuum filtration of 2D materials, such as COF [106], GO [107-111], MXene [112,113], WS_2 [114], MoS_2 [115], suspension on a porous support to construct layer-by-layer deposited membranes. In this method, the 2D nanosheets suspension is slowly filtered onto a desired porous support. Closely packed nanosheets are obtained after filtration that can be readily used in molecular separation tests. Table 5 summarizes the 2D materials based-LNF membranes prepared by vacuum filtration. This kind of 2D materials based-LNF membrane shows an excellent separation performance for textile wastewater treatment and is several orders of magnitude higher than that of the traditional polymer membrane.

GO is the most commonly investigated 2D material for use as the building block of LNF membranes due to its strong hydrophilicity, lamellar structure, and excellent water dispersibility. Conventional GO-based membranes suffer from low water permeance due to the narrow interlayer spacing, and fragile stability in an aqueous environment due to the repulsive hydration force between the functional groups of adjacent GO nanosheets. In order to overcome such two limitations for GO membranes to separate dyes and salts, some approaches, such as crosslinking [109,110], blending [111], and addition of polymer [108] have been tried. For example, Dong et al. [109] fabricated LNF membranes incorporating GO with NH_2-Fe_3O_4 via vacuum filtration, and the resulting membrane exhibited excellent water permeance, which increased from 16.3 to 78 LMH bar^{-1} without losing the dye/salt separation ability (Figure 14). The nano-sized NH_2-Fe_3O_4 can not only adjust the interlayer spacing of GO nanosheets, but also increase the water stability of GO membrane as a crosslinker. Hu et al. [108] selected a surface-initiated atom transfer radical polymerization reaction to design PB-GO LNF membrane through developing a less-charged surface and post chemical crosslinking. The incorporation of sulfonate groups kept the dispersibility of PB-GO in aqueous solution, chemical crosslinking restricted the swelling problem, and pyridine groups improved the antibacterial properties of the resultant LNF membranes.

Table 4
Properties of the LNF membranes prepared by the deposition process.

Membrane materials	Operation pressure	MWCO/pore size	Permeance (LMH bar^{-1})	Dyes rejection	Salts rejection	Ref.
Spray deposition cum post-stabilization technique	2 bar	7900 Da	~25	Methyl blue=99.2% Metani yellow=97.5%		[102]
GO+TA+Ni		-	71.7	Congo red=98.8% Methyl blue=92.9%	Na_2SO_4(1g L^{-1})=5.7% $MgSO_4$(1g L^{-1})=2.4% $MgCl_2$(1g L^{-1})=1.7% NaCl(1g L^{-1})=1%	[94]
PDA/SBMA	4 bar	1580 Da	25	Congo red=98.2% Direct red 23=97.6%	Na_2SO_4(1g L^{-1})=46.2% $MgSO_4$(1g L^{-1})=12.3% $MgCl_2$(1g L^{-1})=1.9% NaCl(1g L^{-1})=8.4%	[101]
polyelectrolytes/PEI/PSS/SB3-14	2 bar	1000 Da	131	Humic acid=99%	NaCl(0.1g L^{-1})=20%	[103]
PSBMA/PDA/MoS_2	1 bar	717 Da, 0.96 nm	262	Methylene blue=99.8%	Na_2SO_4(1g L^{-1})=12.9%	[104]
Catechol/PEI	4 bar	-	24.5	Methyl blue=99.3%	Na_2SO_4(1g L^{-1})=6.2-42.9% NaCl(1g L^{-1})=2.1-22.3%	[99]
EGCg/PEI	2 bar		19	Congo red=99%	Na_2SO_4(1g L^{-1})=4.1%	[98]
Tannic acid/PEI	4 bar	-	40.6	Congo red=99.8%	Na_2SO_4(1g L^{-1})=2.2% NaCl(1g L^{-1})=6.1%	[95]
Gallic acid (GA)/PEI	5 bar		14	Crystal violet=97%	NaCl(1g L^{-1})=20.3%	[97]
PEI-Gallic acid	2 bar	850 Da	25.5	Congo red=97.1% Methyl blue=97.3%	NaCl(1g L^{-1})=2%	[105]
PAN-PEI-TA/PGA	8 bar	3770 Da, 1.32 nm	36.9	Congo red=100% Methyl green=98% Methyl orange=96% Methyl blue=86%	NaCl=14.6%	[96]

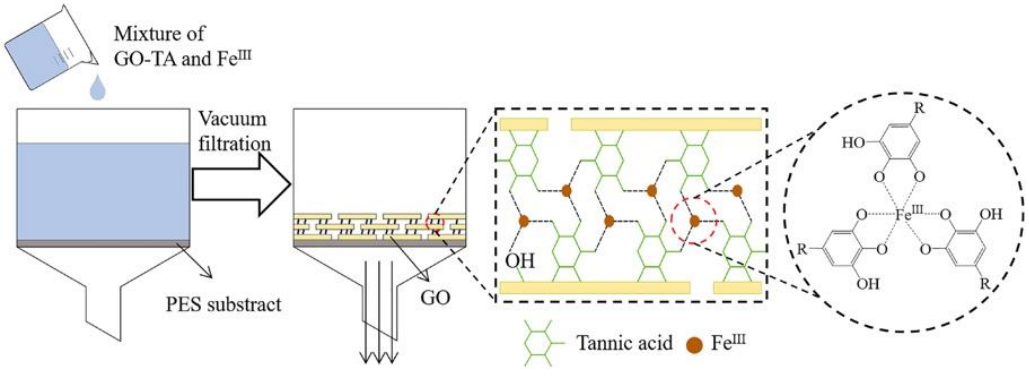

Fig. 13. Schematic of the vacuum filtration process [110],.

Furthermore, 2D COF with a rich tunable structure of nanopores and uniform pore size distribution can provide uniform transport channels for dye/salt separation to achieve excellent permeability and selectivity. Li et al. [106] used a new class of 2D COF nanosheets to construct LNF membranes with precise separation ability via vacuum filtration. The prepared membranes showed exceptionally high water permeance of 141.5 LMH bar^{-1}, while maintaining a high selectivity for dye/salt mixtures. MXene ($Ti_3C_2T_x$) is another type of emerging 2D nanosheets employed as building blocks for LNF membranes due to its rich oxygen-containing groups. Long *et al.* prepared an MXene based LNF membrane with adjustable d-spacing and surface properties [113] through nano-intercalation and vacuum filtration and achieved a superior permeability of 88.8 LMH bar^{-1}. MoS_2, as a newly developed 2D nanosheet, attracted extensive attention for the preparation of LNF membranes due to its smooth surface, low cost, and rigid channels [115]. It should be noted that due to the absence of functional groups on the surface of hydrophobic MoS_2 nanosheets, the membrane prepared based on MoS_2 has poor stability. Moreover, WS_2 with enough rigidity and uniform hydrophilicity has drawn much attention as a promising candidate for constructing LNF membranes [114].

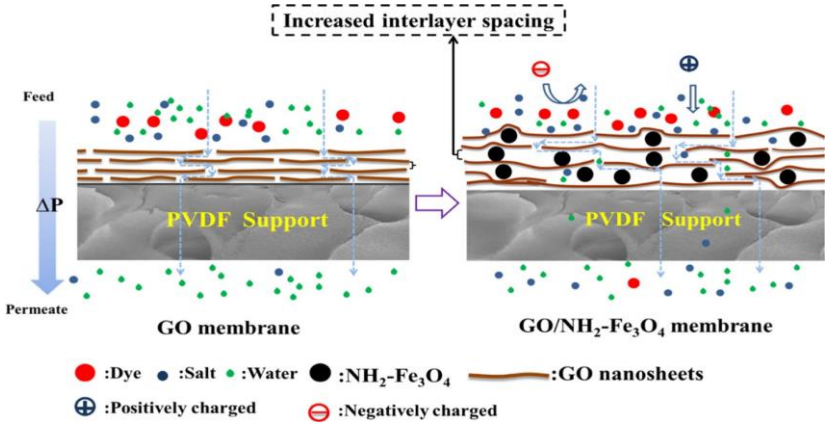

Fig. 14. Schematic representation of GO/NH_2-Fe_3O_4 membrane fabrication [109].

Table 5
Properties of the LNF membranes prepared by vacuum filtration

Membrane materials	Operation pressure	MWCO/pore size	Permeance (LMH bar^{-1})	Dyes rejection	Salts rejection	Ref.
CuTz-1/GO; PVA+GA	4 bar	1750 Da	40.2	Congo red=99.4%	Na_2SO_4(1g L^{-1})=20% $MgSO_4$(1g L^{-1})=8% $MgCl_2$(1g L^{-1})=3% NaCl(1g L^{-1})=0%	[116]
PVDF+GO+Fe3+/Ppy	1 bar	3580 Da	~10	Negative dyes=98.5%	NaCl(1g L^{-1})=~4%	[107]
Melamine/ZnTCPP+TMC	2 bar	3376 Da	63.2	Congo red=99.85% Direct red=98.47% Methyl blue=96.68%	Na_2SO_4(1g L^{-1})=10.1% NaCl(1g L^{-1})=1.6%	[117]
MoS_2@PDA	1 bar	733 Da, 0.5 nm	204.3	Methylene blue=99%	Na_2SO_4=7.6% NaCl=1.3%	[115]
Mxene(Ti3C2Tx)-1D ANF	2 bar	800 Da	195.3	Alcian blue=99.1% Congo red=96.1% Rose bengal=98.6%	NaCl(1-5g L^{-1})=2%	[118]
MXene(Ti3C2Tx)-Al_2O_3	1 bar	637 Da, 0.51 nm	88.8	Rhodamine B>99.5% Methyl blue>99.5%	Na_2SO_4(1g L^{-1})=24% $MgSO_4$(1g L^{-1})=15% NaCl(1g L^{-1})=6%	[113]
PB-GO-GA	2 bar	-	30.3	Congo red>98.3% Direct red 23>98.3% Direct red 80>98.3%	Na_2SO_4(1g L^{-1})<6.9%	[108]
GO/NH_2-Fe_3O_4	5 bar		15.6	Congo red=94%	NaCl(1g L^{-1})=15%	[109]
Fe/GO-TA20	1 bar	0.8~1.5 nm	61.2	Congo red>99% Methyl blue>99% Evans blue>99%	NaCl(1g L^{-1})=6%	[110]
A-HNTs/GO	0.9 bar	-	159.4	Methyl orange=92.98% Methylene blue=92.86%	Na_2SO_4(1g L^{-1})=15.2% $MgSO_4$(1g L^{-1})=15.2% $MgCl_2$(1g L^{-1})=5.1% NaCl(1g L^{-1})=8.9%	[111]
WS_2+PA	1 bar		597	Rose bengal=98.5%	NaCl(1.2-60g L^{-1})=0.3%	[114]
2D-CTF-1	1 bar	1.39 nm	141.5	Congo red=97.6%		[106]
DES/GO	3 bar	-	124.8	Alcian blue=99.6% Brilliant blue=99.3% Methyl blue=92.2% Rhodanile blue=89.9%	Na_2SO_4(1g L^{-1})=18.1%	[119]

3.5. Others

In addition to the aforementioned commonly used methods for manufacturing LNF membranes, other researchers use graft polymerization [120-122], chemical crosslinking [123-127], layer by layer [128-130], electrostatic complexation [131-134], in situ growth [135-137] to prepare LNF membranes, as concluded in Table 6. Graft polymerization is a method for preparing LNF membranes by connecting target compounds on the membrane surface through a chemical reaction. Graft modification has the advantage of allowing the properties of the graft layer to be adjusted by selecting different monomers and polymers, so it is also widely utilized to prepare LNF membranes. Guo et al. [122] obtained zwitterionic LNF membranes by reacting 1, 3-propane sultone with a polyamide selective layer via grafting reaction. The zwitterionic LNF membranes display reduced monovalent salt rejection compared with pristine polyamide membranes due to the introduction of zwitterions, which can penetrate monovalent ions through strong electrostatic attractions. Although some progress has been made in the preparation of LNF membranes by surface grafting, it is still not suitable for practical production in consideration of the production cost, the difficulty of the operation, and the poor performance of prepared membranes [120,121].

Layer-by-layer (LBL) assembly is a method of forming nanoscale selective layers by depositing one or more molecules on the carrier's surface in a certain order using intermolecular interactions such as electrostatic contact, hydrogen bonds, coordination bonds, etc. [128-130]. In this procedure, the progressive deposition of molecules is commonly accomplished by alternating soaking and washing. As shown in Figure 15, Ma's group ascribed the separation performance enhancements for both cationic and anionic molecules by dually charged LNF membranes to alternately charged sandwich structures because a mono-charged selective layer tends to be compromised by the opposite-charged foulants [130]. The polyelectrolyte LNF membranes prepared by the LBL method still have limitations in practical applications, such as poor stability under high ionic strength, because salt ions easily permeate the multilayer membrane and shield the polyelectrolyte charge. Therefore, Liu et al. [129] introduced WS_2 into a polyelectrolyte membrane through coordinate-bond-reinforcement to enhance the stability and antifouling performance of the LBL LNF membrane. To overcome the complexity and time-consuming limitation of the LBL method, a bottom-up electrostatic self-assembly method with low cost and high efficiency is a good alternative for the preparation of LNF membranes. Zhao et al. [133] used PEI as a chelating agent and Co^{2+} as a metal ion with a post-treatment for the in-situ formation of Ni/Co layered double hydroxides to form an LNF membrane with excellent dye desalination performance. To achieve a straightforward methodology for preparing LNF membranes, alginate was introduced into the chelation self-assembly process between PEI and metal ions, realizing the purpose of designing high-performance LNF membranes without post-treatment, since the alginate coating achieved by electrostatic interaction does not require any functionalization [134]. However, the PEI/metal ions LNF membranes will suffer severe structural deterioration under alkaline or acidic conditions due to non-covalent interactions sensitive to the external environment. Jiang's group designed fluorinated membranes via electrostatic complexation inspired by sandcastle worms. The resultant LNF membrane with the excellent antifouling performance showed superior water permeance of 93.3 LMH bar^{-1} and high dye rejection of over 90% [132]. The long-term stability of the loosely assembled LNF membrane fabricated by LBL or electrostatic complexation in a harsh environment, such as strong acidic, alkaline, and ionic conditions, is questionable; thus, the combination of the two methods mentioned above with crosslinking has recently been shown to be a promising approach to obtain desirable LNF membrane to overcome its latent instability. For example, PEI and phosphorylated PEI are assembled via electrostatic complexation, followed by glutaraldehyde crosslinking [126], which endows the resultant LNF membrane with high permeability (24.2 LMH bar^{-1}) and excellent stability in a broad pH range.

For both high permeability and high selectivity for the treatment of textile wastewater, LNF membranes with tunable order nanopores are an ideal choice. Today, metal-organic frameworks (MOFs) and covalent-organic frameworks (COFs) have emerged to construct composite LNF membranes via the in-situ growth method [135-137], demonstrating extraordinary performances for molecular-level separations due to their well-defined structure. Furthermore, eco-friendly, low-cost hydrogel membranes show excellent performance in the treatment of textile wastewater, providing a new idea for the design of next-generation LNF membranes [138,139].

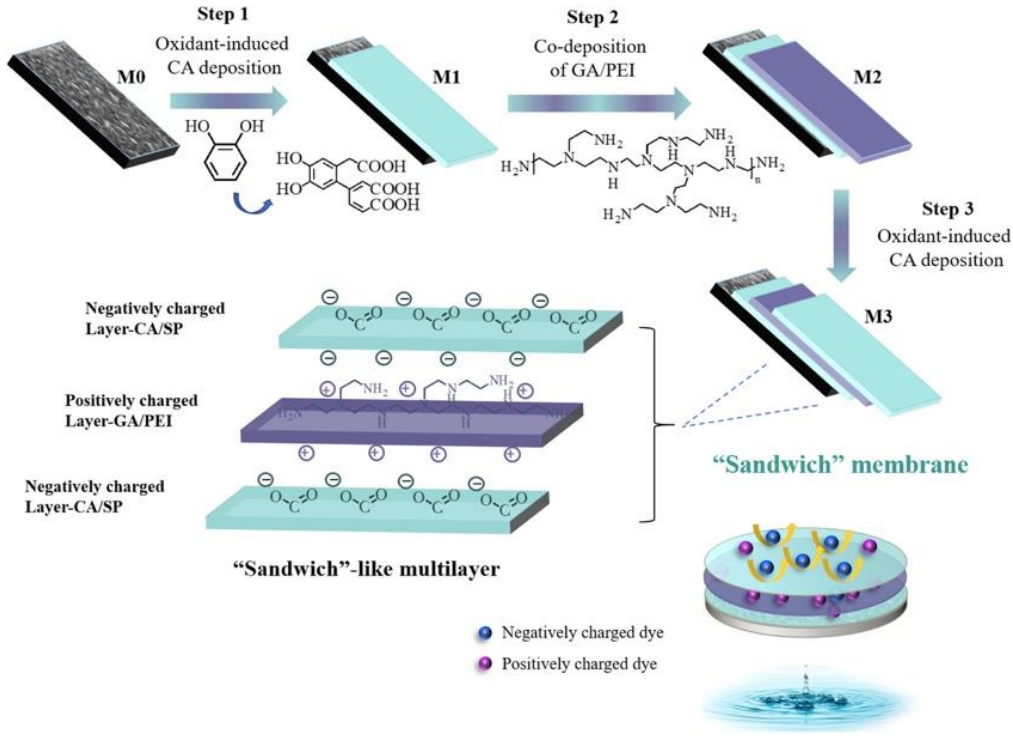

Fig. 15. Schematic illustration of fabrication process of the LBL method [130].

Table 6
Properties of the LNF membranes prepared by other methods.

Membrane materials	Operation pressure	MWCO/pore size	Permeance (LMH bar^{-1})	Dyes rejection	Salts rejection	Ref.
Graft polymerization						
GO/DTiO$_2$-PDA-PEI	7 bar	0.87 nm	41.6	Eriochrome black T=99.9% Congo red=99.6%	NaCl(2g L^{-1})=0.36% Na_2SO_4(1g L^{-1})=4.8%	[120]
Catechin, chitosan	2 bar	720 Da, 1.24 nm	7.2	Acid fuchsin=98.7% Crystal violet=98.5%	$MgSO_4$(1g L^{-1})=15.8% $MgCl_2$(1g L^{-1})=16.2% NaCl(1g L^{-1})=12.5%	[121]
DEEDA/1,3-PS	6 bar	350 Da	14.6	Antibiotics>95%	NaCl(1g L^{-1})<10%	[122]
Chemical crosslinking						
PVDF/SMA+PEI+EGDGE		0.94 nm	6.4	Methyl orange=99.75%	Na_2SO_4<15%	[123]
PVDF/SMA-PEI-Cu^{2+}	1 bar	1615 Da	26.2	Crystal violet=96.1 Sunset yellow=99.6	Na_2SO_4(1g L^{-1})=9.4%	[124]
Chitosan-helical carbon-SDS	3 bar		20	Organic molecule=99.8%	Sal(2g L^{-1})t=8%	[125]
PEI-PO_3Na/PEI	2 bar	1.22 nm	24.2	Victoria blue bo=99.5%	NaCl(1g L^{-1})=10.1%	[126]
GO+CNT	1 bar		26.3	Congo red=98.7% Methyl blue=94.6%	Na_2SO_4=6.3% NaCl=3.1%	[127]
Layer by layer (LBL)						
8NH_3Cl-POSS+TA	4 bar	440 Da	21	Antibiotics>95.1%	NaCl(1g L^{-1})=7%	[128]
WS_2+polyelectrolytes	6 bar	1182 Da	34.3	Reactive black 5>99%	NaC=10%	[129]
CA-GA/PEI/CA	1.5 bar	5.85 nm	~20	Alcian blue=99.6% Brilliant blue=99.3% Methyl blue=92.2% Rhodanile blue=89.9%		[130]
Electrostatic complexation						
Ag^+-PEI/ Cu^{2+}-PEI/ Fe^{3+}-PEI	4 bar	420 Da	12.1	Acid fuchsin=96.5%	$MgSO_4$(1g L^{-1})=31.5%	[131]
PA-QCL-PFSA	1 bar	1.59 nm	93.3	Organic dyes (>450 Da) >90%	Salts<10%	[132]
Co/Ni LDHs/PEI	2 bar		19.8	Acid fuchsin=97.5% Methyl blue=97.9%	NaCl(1g L^{-1})<3%	[133]
PAI/PEI-Alg-Fe^{3+}		1297 Da	25	Methyl green>97%	NaCl(1g L^{-1})=3%	[134]
Hydrogel membrane						
TiO$_2$-COOH/CaAlg	1 bar	0.32 nm	14.4	Brilliant blue G250=98.4% Direct black 38=96.8% Congo red=95.9%	Na_2SO_4(1g L^{-1})=15.6% $MgSO_4$(1g L^{-1})=16.1% $MgCl_2$(1g L^{-1})=12.3% NaCl(1g L^{-1})=9%	[139]
CaAlg-PP	1 bar	650 Da	20.3	Methyl blue=100%	NaCl(0.5g L^{-1})=7.5%	[138]
In-situ growth						
POP-PAN	4 bar	6000 Da, 1.95 nm	66.5	Congo red=99.6% Direct red 23=98% Methyl blue=98.8%	Salts<15%	[135]
ZIF-8+GO	1 bar	1300 Da, 1 nm	60	Methyl blue=100%		[136]
COF-300	5 bar	410 Da	79	Chrome black T=97.4%		[137]

Table 7 summarizes the previously discussed methods for preparing LNF membranes. Each method proposed has its unique advantages, among which IP, NIPS, and vacuum filtration are the most appropriate for industrial applications. Furthermore, one of the key research topics in the further will be the vacuum filtration method for preparing ultra-high performance 2D materials-based LNF membranes.

4. Membrane fouling and control strategies

4.1. Formation of membrane fouling

Membrane fouling is a major stumbling block for applications of LNF membranes. Membrane fouling occurs when foulants in the feed solutions, such as inorganic salts, organic molecules, colloids, bacteria deposit on the membrane surface or block the membrane pores during real operation, leading to a reversible or irreversible decline in water flux and selectivity [140]. As indicated in Figure 16, it can be classified as inorganic fouling, organic fouling, colloidal fouling, or biofouling, depending on the type of foulant. Inorganic fouling is mainly produced by inorganic salts that are slightly soluble and easy to scale, such as carbonate and silicate. The concentration of inorganic contaminants in the feed solution rises as the separation proceeds. When the solubility is surpassed, scale forms on the membrane surface, causing the blockage of membrane pores. Organic pollutants mainly deposit on the membrane surface in the way of adsorption to form a relatively stable filter cake layer, and the fouling degree is determined by interactions between the membrane surface and pollutants, such as hydrophobic force, electrostatic force, hydrogen bond force, etc. [141]. Colloidal fouling is primarily caused by colloidal particles deposited on the membrane surface, such as silica, sulfur, iron, silt, and natural organic matter. Some high molecular weight proteins and polysaccharides can also be classified as colloidal pollutants. Biofouling is caused by bacterial, fungi, microbial cells, and extracellular polymers [142]. These living active objects deposit on the membrane surface and form a reproductive biofilm, which then causes membrane fouling. Biofilms are extremely viscous and difficult to clean. Special cleaning methods such as acid, alkali, surface activator, or biological enzyme are generally used to destroy the biofilms and restore water flux.

Table 7
Advantages of the different LNF membrane fabrication methods.

Technique	Advantages
Interfacial polymerization	Utilized at an industrial scale Large scale production Low cost High reproducibility Facile and effective approach High filtration performance
Nonsolvent induced phase separation	Utilized at industrial scale Large scale production Low cost High reproducibility Versatile membrane thickness
Bio-inspired deposition	Tunable surface chemistry Improved hydrophobicity Gentle precipitation condition Modification of various materials
Vacuum filtration	Inexpensive Simple to scale up 2D materials based LNF membranes Excellent separation performance
Graft polymerization Chemical crosslinking Layer by layer Electrostatic complexation Hydrogel membrane In-situ growth	Tunable surface properties

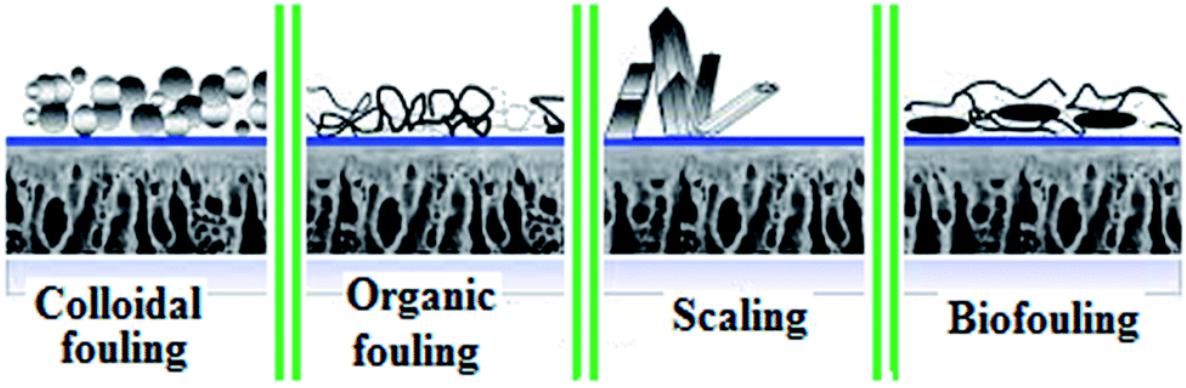

Fig. 16. Types of membrane fouling [140].

As shown in Figure 17, the specific process of membrane fouling can be divided into three stages [143]. The first stage is the concentration polarization stage. When the feed solution contacts the membrane surface, the solute molecules of larger size are selectively trapped on the membrane surface by the selective layer. If the flow rate on the membrane surface is low and not sufficient to disperse solutes back to the feed solution in time, the solute concentration on the membrane surface becomes higher than that of the feed solution. In the second stage, the macromolecular solutes are trapped and deposited on the membrane surface to form a gel layer, while small molecular solutes will enter the membrane pores and be adsorbed on the pore walls, resulting in a significant decrease in membrane separation performance. Finally, with the process of membrane separation, solute deposition and diffusion on the membrane surface reach a dynamic balance, and the decreasing trend of membrane separation performance gradually stabilizes. Textile wastewater contains complex anionic dyes, cationic dyes, dyeing auxiliaries, etc. The membrane easily adsorbs organic matter in the wastewater during operation, resulting in membrane organic fouling and biofouling. Therefore, the research and development of LNF membranes with high permeability selectivity and excellent fouling resistance for textile wastewater treatment have significant research implications and applications.

4.2. Strategies for improving LNF membrane fouling resistance

Membrane fouling is unavoidable during the filtration process, but its impact can be minimized. To deal with membrane fouling, various approaches and protocols have been employed. It is difficult to alleviate membrane fouling fundamentally by adjusting external operating parameters. Therefore, one should start from the membrane itself to develop new LNF membranes with excellent antifouling performance and self-cleaning ability to fundamentally alleviate the problem of membrane fouling. The construction of antifouling surface mainly from improving the hydrophilicity of membrane surface, reducing surface roughness, and regulating the surface charge properties. Furthermore, antibacterial and photocatalytic compounds are being used in LNF membranes to provide them antibacterial qualities and self-cleaning capabilities.

As shown in Figure 18, researchers have focused on three features of LNF membranes to increase their antifouling ability: enhancing hydrophilicity, lowering roughness, and regulating surface charge [140,142,143]. These three aspects are also the most visible manifestations of membrane surface properties, and they influence pollutant deposition on the membrane surface in various ways. Generally speaking, as the hydrophobicity of the membrane surface increases, the contaminants are drawn towards the membrane surface by hydrophobic forces and finally deposit. As a result, increasing the hydrophilicity of the membrane surface makes it easier for the membrane surface to combine with water molecules to form a hydration layer, which effectively reduces the hydrophobic force and prevents contaminants between pollutants and the membrane surface. Graphene quantum dots (GQDs) [54,59,60] and carbon quantum dots (CQDs) [56-58] with hydrophilic hydroxyl and carboxyl groups exhibit good dispersion and compatibility with the selective layer of LNF membranes. In this context, the manufactured LNF membranes with high permeability and fouling resistance brought on by CQDs and GQDs doping can be predicted to help fractionate dye/salt mixtures. Roughness is another important surface property that affects membrane fouling. Pollutants easily accumulate in depressions on the membrane surface to form an interlocking structure. When the pollutants accumulate to a certain extent, it is difficult for the shear force of water flow to reach the depression, resulting in a lower flux recovery rate after cleaning the membrane, especially when the size of the pollutants is equivalent to the surface roughness of the membrane, the accumulation trend of pollutants on the membrane surface is more obvious. The surface functional groups on the membrane surface tend to be ionized and the membrane surface is charged when it comes into contact with an aqueous solution with a specific pH value. When the charge of the pollutants is opposite to the charge of the membrane surface, under the action of strong static electricity, foulants are adsorbed on the membrane surface in significant amounts, resulting in membrane fouling. On the contrary, when the foulant charge is the same as the membrane surface charge, electrostatic repulsion reduces adsorption and has an antifouling effect. The neutral charge surface has been extensively explored in recent years, showing good antifouling properties [79,101,103]. The typical neutral charge surface is constructed by a zwitterionic surface. A zwitterionic polymer is a neutral polymer containing both cations and anions. The strong hydration ability of zwitterionic polymers can reduce the adsorption of organic matter and improve the antifouling ability of LNF membranes.

One of the biggest stumbling blocks to maintaining a high-efficiency separation and water treatment stability is the growth and reproduction of microorganisms on the surface of LNF membranes. Extracellular polymeric substances have a strong protective effect on bacteria, making physical and chemical cleaning of membrane surfaces difficult once a mature biofilm has been established [144]. Therefore, by restricting the growth and reproduction of initial bacterial cells on the membrane surface, the construction of an antibacterial membrane surface can lower the likelihood of biofilm formation, thereby achieving the purpose of enhancing biofouling resistance.

Previous intensive research focused on constructing antibacterial LNF membranes via adding leachable nanoparticles [99,116,131,145] onto the membrane surface and anchoring biocidal polymers [97,101] for contact killing to solve the challenges listed above. For example, Gao et al. [131] constructed LNF membranes with antibacterial activity for dye recycling via electrostatic self-assembly, as shown in Figure 19. The chelation of metal ions (Ag^{+}/Cu^{2+}/Fe^{3+}) and PEI endow the membrane with antibacterial ability, and the resultant LNF membrane achieved high water permeance and efficient fractionation of dye/salt mixture. Li et al. [101] used a zwitterionic polymer with dopamine to prepare LNF membranes with excellent antibacterial properties.

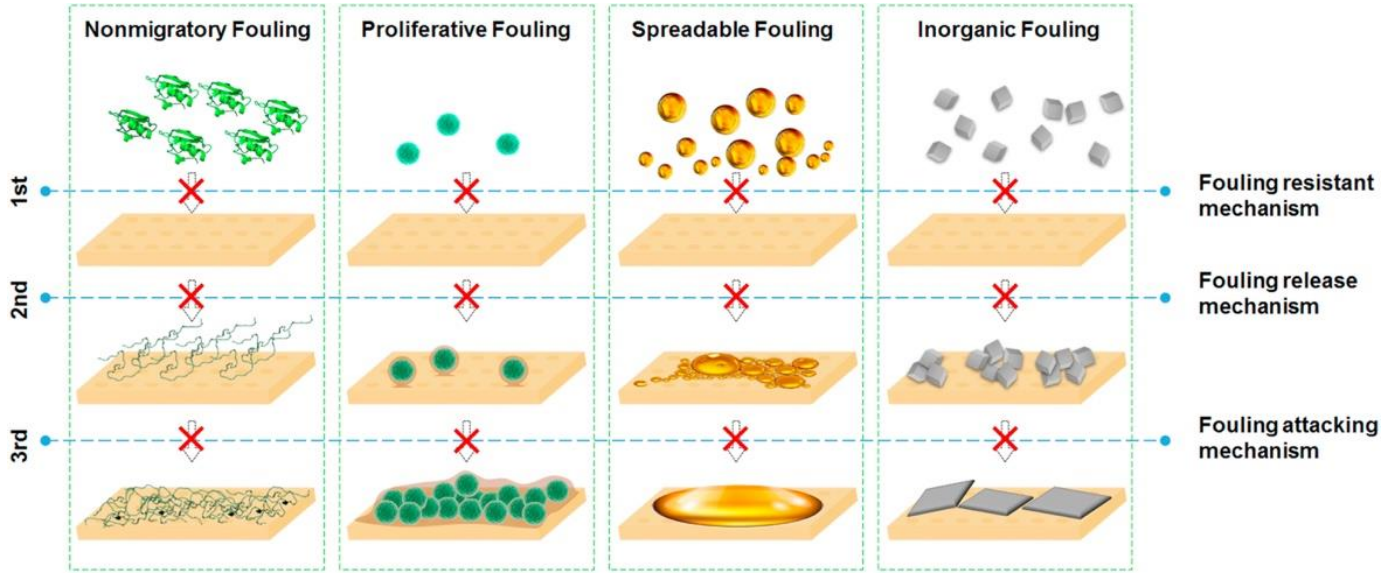

Fig. 17. Schematics of the three-stage membrane fouling behaviors and proposed antifouling mechanisms [143].

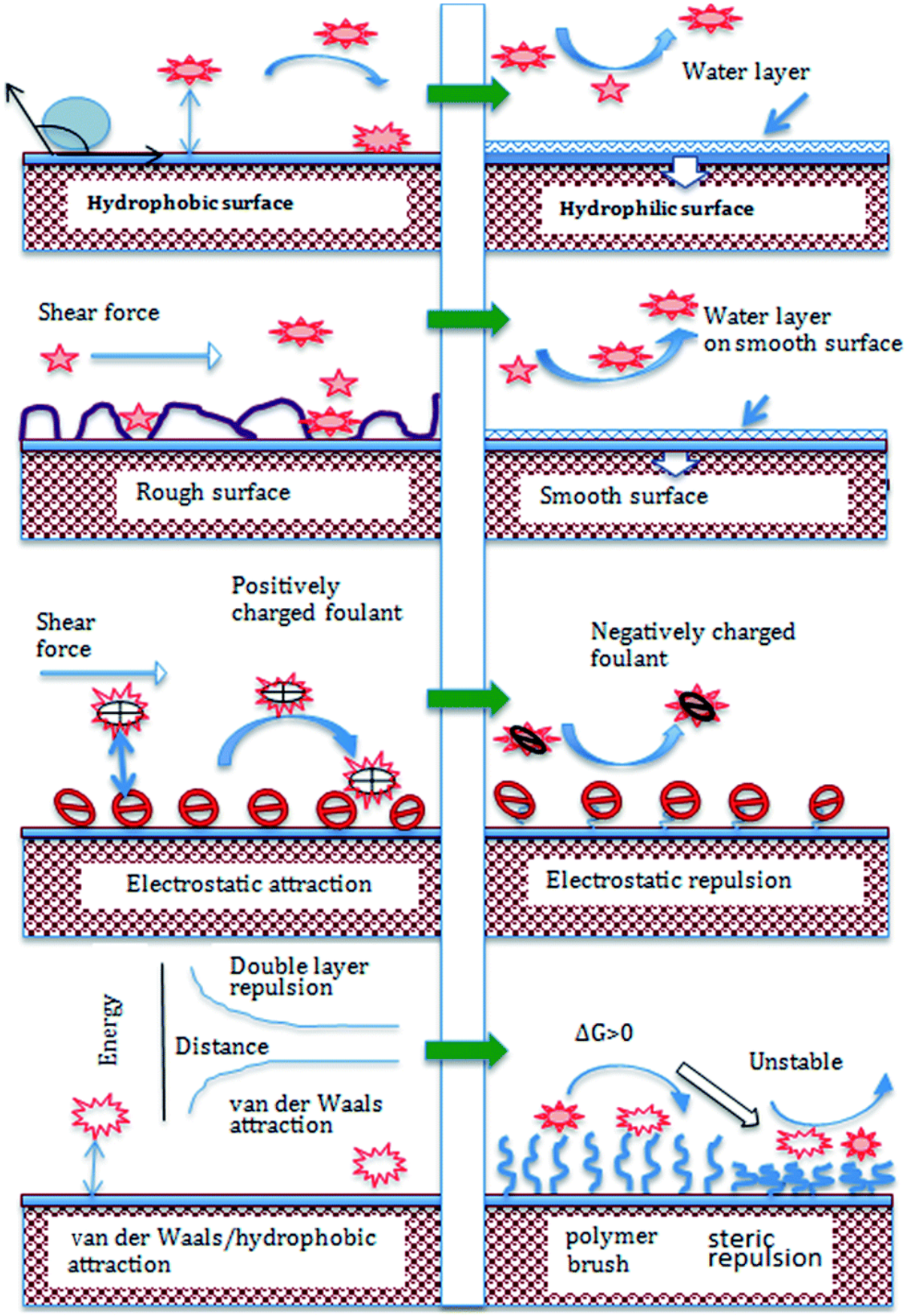

Fig. 18. Membrane surface properties and their correlation with membrane fouling and antifouling [140].

Furthermore, LNF membrane photocatalysis, which has the ability to degrade dyes while also allowing for self-cleaning, has emerged as the most cutting-edge research in the field of textile wastewater treatment [146]. The irreversible dye fouling induced by the hydrophobic and electrostatic interaction between dye molecules and membrane surface can be greatly reduced by this self-cleaning capacity, as shown in Figure 20. Photocatalysis is an appealing and sustainable approach for decomposing pollutants, because it is environmentally beneficial, utilizes potential sunlight as an energy source, and the photocatalytic products are frequently harmless [147]. After years of modest development and skepticism, the integration of photocatalysis, such as TiO_2 nanoparticles, g-C_3N_4, MOFs, and COFs, into LNF membrane processes is emerging as a potential option for membrane fouling alleviation [116,117,146,148,149]. Zhang and Zhu's group conducted a series of studies on photocatalysis to give LNF membranes self-cleaning ability for textile wastewater treatment. They constructed a copper-triazolate MOFs (CuTz-1)/GO composite membrane with favorable photocatalytic and antimicrobial properties via vacuum filtration followed by chemical crosslinking. The pure water permeance was up to 40.2 LMH bar^{-1}, the rejections of various dyes were higher than 95%, and the rejection of NaCl is as low as 0.3% [116]. Then they dispersed photocatalytic Zn-TCPP in melamine aqueous phase and TMC organic phase via IP to obtain Zn-TCPP embedded TFN membrane with dye degradation ability under visible light [117]. Furthermore, Meng et al. [148] fabricated visible light catalytic NF membranes via in situ synthesis $AgBr-Ag_3PO_4$ on the surface of NF membranes composited by TA and TDI monomers. Even though the resultant membrane did not achieve high water permeance or effective dye/salt separation, it did a decent job of degrading Congo red, with 85% degradation achieved after four cycles.

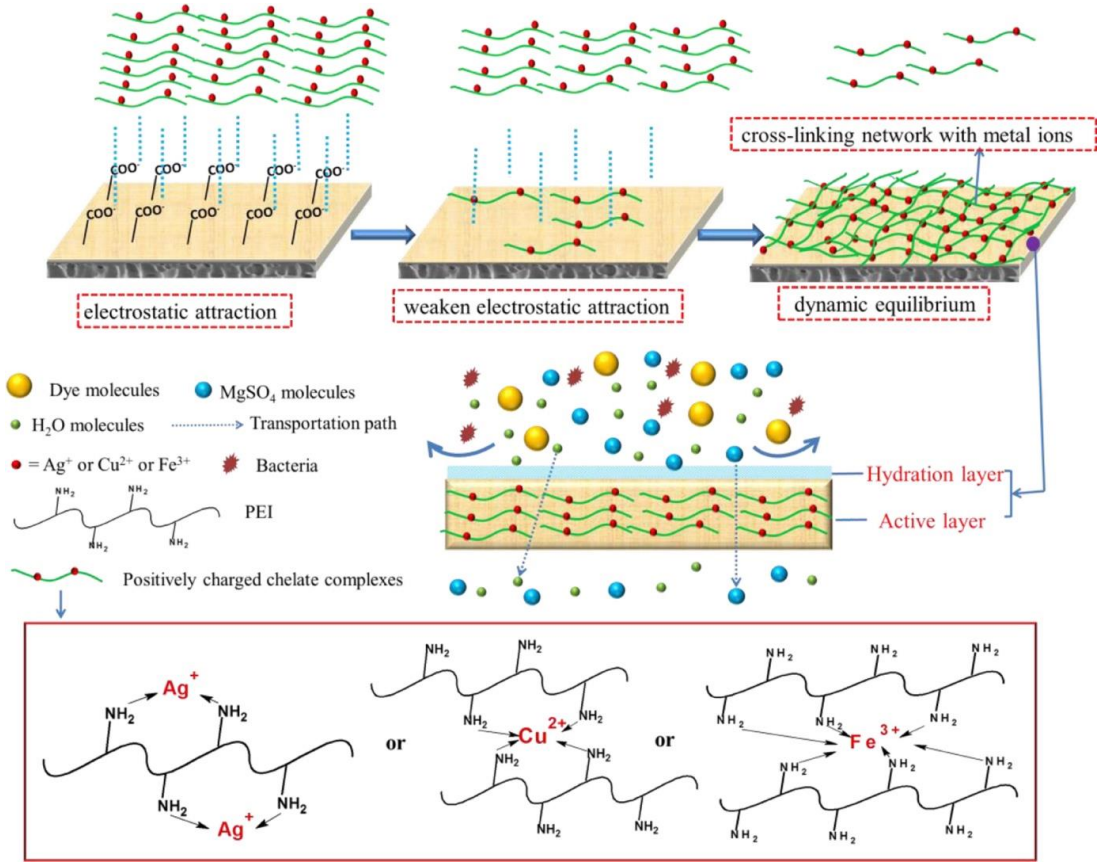

Fig. 19. Schematic diagram of reactants, membrane preparation, and dye/salt mixture separation [131].

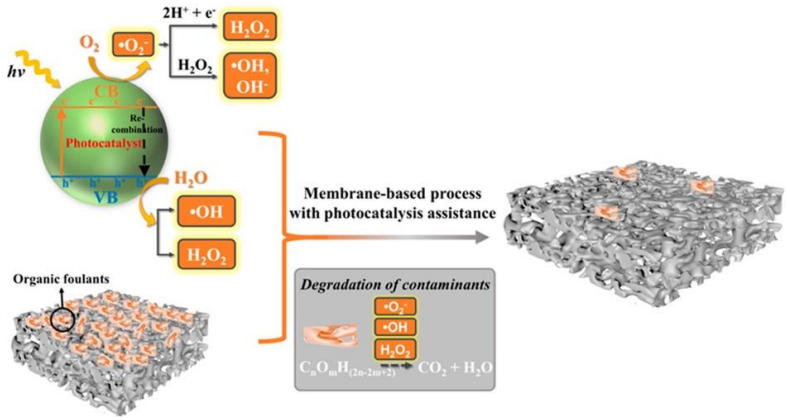

Fig. 20. Schematic mechanism of photocatalytic degradation of contaminants and its application potential in membrane fouling control [146].

5. Conclusion and outlook

Compared with NF membranes, LNF membranes with higher permeability, lower salt rejection, and higher selectivity for dye/salt mixtures show great advantages in resource recovery from textile wastewater. Researchers have been particularly interested in the fabrication of LNF membranes with great selectivity and outstanding antifouling performance based on the unambiguous separation mechanism of LNF. This review paper attempts to summarize the separation mechanism of LNF for textile wastewater, the cutting-edge high-performance LNF membrane preparation methods, and the strategy for constructing LNF membrane with excellent antifouling performance. Researchers have conducted extensive research on the selective separation mechanism of LNF membranes and proposed corresponding separation mechanisms that can explain the separation process of LNF membranes in terms of size sieving and electrostatic repulsion. However, there are still some controversies, and further exploration needs to combine the features of the membrane material with the characteristics of dye molecules, as well as the feed solution.

Various methods have been employed for the fabrication of LNF membranes, such as IP, NIPS, bio-inspired deposition, and vacuum filtration. Among these methods, IP technology, as the extensively used NF membrane preparation method in the world, is still the most promising technology for preparing high-performance LNF membranes. Recently, polyester LNF membranes with a loose structure and high hydrophilicity and COF-based LNF membranes with regular and adjustable pore size prepared via IP have shown high permeability while maintaining a competitive selectivity. However, the usage of polyester and COF- based LNF membranes in harsh environments, such as strong acid, alkali, and bacterial contamination, is limited due to the lack of strong alkali resistance for polyester film and strong COF adsorption for organic solutes. Therefore, it will be necessary to build LNF membranes with stable chemical properties, acid and alkali resistance, and certain antibacterial effects based on the IP approach. In recent years, LNF membranes prepared by vacuum filtration with 2D nanosheets have shown great potential in the treatment of textile wastewater. This kind of LNF membrane can easily integrate ultra-high water permeance, antifouling, antibacterial, and self-cleaning functions, the only drawback is the difficulty of large-scale fabrication. Although the performance of LNF membranes prepared by NIPS and bio-inspired deposition is not outstanding, these two methods are the simplest to provide LNF membranes with special functionality.

Most LNF membranes are still on a lab scale. So far, using LNF membranes to treat textile wastewater while meeting strict environmental regulations is still a huge challenge. Due to membrane fouling, LNF membrane technology is inevitably affected by the decline in flux. Improving the antifouling performance of LNF membranes has emerged as one of the most pressing issues in the treatment of textile wastewater. Based on the deep understanding of membrane fouling mechanisms, research on the construction of antifouling LNF membranes mainly focuses on the regulation of membrane surface structure-performance relationships, such as hydrophilicity-fouling resistance, biotoxicity-antibacterial property, photocatalyst-self-cleaning. The antifouling surface can be constructed by improving the hydrophilicity of the LNF membrane surface. CQDs, GQDs, and zwitterions are currently the most researched substances. The introduction of biocidal agents can effectively inhibit the formation of biofilms, and thus endows the LNF membrane with antibacterial ability. Furthermore, combining photocatalysts into LNF membranes is a promising environmentally friendly method for membrane fouling mitigation. Some efforts have been made to improve the ability of LNF membranes to photocatalytic degradation of dyes under visible light, thus achieving self-cleaning ability.

On the basis of an extensive literature review, we summarize some current research challenges and possible solutions. There are mature mass transfer and separation mechanisms of the NF process, but LNF is somehow different from traditional NF due to its high salt permeability. Therefore, further experiments and theoretical analysis are needed to explore the separation mechanisms that govern LNF. A simple preparation procedure and cheap cost are unquestionably required to produce commercial LNF membranes. Therefore, IP technology seems to be the most promising method to prepare excellent commercial LNF membranes through monomer selection, pore size control, changing charge properties. Under severe solutions conditions, LNF composed of 2D nanosheets has the potential to exhibit chemical stability and resistance to acids and alkalis. In addition, 2D nanosheets are also one of the sources of biocidal agents and photocatalytic materials. Therefore, 2D nanosheets-based LNF membranes have the potential to combine fouling resistance and fouling attacking to achieve functional diversity. The above-mentioned issues should be the focus of future research.

Acknowledgments

Pengrui Jin would like to acknowledge the support provided by the China Scholarship Council (CSC) of the Ministry of Education, P.R. China (CSC No. 201806050043)

References

[1] J. Lin, W. Ye, H. Zeng, H. Yang, J. Shen, S. Darvishmanesh, P. Luis, A. Sotto, B. Van der Bruggen, Fractionation of direct dyes and salts in aqueous solution using loose nanofiltration membranes, J. Membr. Sci., 477 (2015) 183-193. https://doi.org/10.1016/j.memsci.2014.12.008

[2] C. Xue, Q. Chen, Y.-Y. Liu, Y.-L. Yang, D. Xu, L. Xue, W.-M. Zhang, Acid blue 9 desalting using electrodialysis, J. Membr. Sci., 493 (2015) 28-36. https://doi.org/10.1016/j.memsci.2015.06.027

[3] M. Erkanlı, L. Yilmaz, P.Z. Culfaz-Emecen, U. Yetis, Brackish water recovery from reactive dyeing wastewater via ultrafiltration, J. Clean. Prod., 165 (2017) 1204-1214. https://doi.org/10.1016/j.jclepro.2017.07.195

[4] S. Yu, C. Gao, H. Su, M. Liu, Nanofiltration used for desalination and concentration in dye production, Desalination, 140 (2001) 97-100. https://doi.org/10.1016/S0011-9164(01)00358-7

[5] D. Yaseen, M. Scholz, Textile dye wastewater characteristics and constituents of synthetic effluents: a critical review, Int. J. Environ. Sci. Technol., 16 (2019) 1193-1226. https://doi.org/10.1007/s13762-018-2130-z

[6] S. Arslan, M. Eyvaz, E. Gürbulak, E. Yüksel, A review of state-of-the-art technologies in dye-containing wastewater treatment–the textile industry case, Textile wastewater treatment, (2016) 1-29. https://doi.org/10.5772/64140

[7] J. Chen, Q. Wang, Z. Hua, G. Du, Research and application of biotechnology in textile industries in China, Enzyme Microb. Technol., 40 (2007) 1651-1655. https://doi.org/10.1016/j.enzmictec.2006.07.040

[8] T.W. Seow, C.K. Lim, Removal of dye by adsorption: a review, J. bioremediat. biodegrad., 11 (2016) 2675-2679. https://doi.org/10.4172/2155-6199.1000371

[9] J. Dotto, M.R. Fagundes-Klen, M.T. Veit, S.M. Palacio, R. Bergamasco, Performance of different coagulants in the coagulation/flocculation process of textile wastewater, J. Clean. Prod., 208 (2019) 656-665. https://doi.org/10.1016/j.jclepro.2018.10.112

[10] J. Dasgupta, J. Sikder, S. Chakraborty, S. Curcio, E. Drioli, Remediation of textile effluents by membrane based treatment techniques: a state of the art review, J. Environ. Manage., 147 (2015) 55-72. https://doi.org/10.1016/j.jenvman.2014.08.008

[11] B. Bethi, S.H. Sonawane, B.A. Bhanvase, S.P. Gumfekar, Nanomaterials-based advanced oxidation processes for wastewater treatment: a review, Chem. Eng. Process., 109 (2016) 178-189. https://doi.org/10.1016/j.cep.2016.08.016

[12] M. Rochkind, S. Pasternak, Y. Paz, Using dyes for evaluating photocatalytic properties: a critical review, Molecules, 20 (2015) 88-110. https://doi.org/10.3390/molecules20010088

[13] K. Sarayu, S. Sandhya, Current technologies for biological treatment of textile wastewater–a review, Appl. Biochem. Biotechnol., 167 (2012) 645-661. https://doi.org/10.1007/s12010-012-9716-6

[14] R. Shoukat, S.J. Khan, Y. Jamal, Hybrid anaerobic-aerobic biological treatment for real textile wastewater, Journal of Water Process Engineering, 29 (2019) 100804. https://doi.org/10.1016/j.jwpe.2019.100804

[15] V. Jegatheesan, B.K. Pramanik, J. Chen, D. Navaratna, C.-Y. Chang, L. Shu, Treatment of textile wastewater with membrane bioreactor: a critical review, Bioresour. Technol., 204 (2016) 202-212. https://doi.org/10.1016/j.biortech.2016.01.006

[16] K. Paździor, L. Bilińska, S. Ledakowicz, A review of the existing and emerging technologies in the combination of AOPs and biological processes in industrial textile wastewater treatment, Chem. Eng. J., 376 (2019) 120597. https://doi.org/10.1016/j.cej.2018.12.057

[17] M. Al-Mamun, S. Kader, M. Islam, M. Khan, Photocatalytic activity improvement and application of UV-TiO2 photocatalysis in textile wastewater treatment: A review, J. Environ. Chem. Eng., 7 (2019) 103248. https://doi.org/10.1016/j.jece.2019.103248

[18] R. Epsztein, R.M. DuChanois, C.L. Ritt, A. Noy, M. Elimelech, Towards single-species selectivity of membranes with subnanometre pores, Nat. Nanotechnol., 15 (2020) 426-436. https://doi.org/10.1038/s41565-020-0713-6

[19] J.R. Werber, C.O. Osuji, M. Elimelech, Materials for next-generation desalination and water purification membranes, Nat. Rev. Mater., 1 (2016) 1-15. https://doi.org/10.1038/natrevmats.2016.18

[20] B. Van der Bruggen, Sustainable implementation of innovative technologies for water purification, Nat. Rev. Mater., 5 (2021) 217-218. https://doi.org/10.1038/s41570-021-00264-7

[21] B. Freeman, Y. Yampolskii, I. Pinnau, Materials science of membranes for gas and vapor separation, John Wiley & Sons, 2006. https://doi.org/10.1002/047002903X

[22] A.W. Mohammad, Y. Teow, W. Ang, Y. Chung, D. Oatley-Radcliffe, N. Hilal, Nanofiltration membranes review: Recent advances and future prospects, Desalination, 356 (2015) 226-254. https://doi.org/10.1016/j.desal.2014.10.043

[23] Y. Liang, Y. Zhu, C. Liu, K.-R. Lee, W.-S. Hung, Z. Wang, Y. Li, M. Elimelech, J. Jin, S. Lin, Polyamide nanofiltration membrane with highly uniform sub-nanometre

pores for sub-1 Å precision separation, Nat. Commun., 11 (2020) 1-9. https://doi.org/10.1038/s41467-020-15771-2

[24] Y. Zhao, T. Tong, X. Wang, S. Lin, E.M. Reid, Y. Chen, Differentiating Solutes with Precise Nanofiltration for Next Generation Environmental Separations: A Review, Environ. Sci. Technol., 55 (2021) 1359-1376. https://doi.org/10.1021/acs.est.0c04593

[25] S. Guo, Y. Wan, X. Chen, J. Luo, Loose nanofiltration membrane custom-tailored for resource recovery, Chem. Eng. J., (2020) 127376. https://doi.org/10.1016/j.cej.2020.127376

[26] B. Van der Bruggen, E. Curcio, E. Drioli, Process intensification in the textile industry: the role of membrane technology, J. Environ. Manage., 73 (2004) 267-274. https://doi.org/10.1016/j.jenvman.2004.07.007

[27] C.-Z. Liang, S.-P. Sun, F.-Y. Li, Y.-K. Ong, T.-S. Chung, Treatment of highly concentrated wastewater containing multiple synthetic dyes by a combined process of coagulation/flocculation and nanofiltration, J. Membr. Sci., 469 (2014) 306-315. https://doi.org/10.1016/j.memsci.2014.06.057

[28] C.-Z. Liang, S.-P. Sun, B.-W. Zhao, T.-S. Chung, Integration of Nanofiltration Hollow Fiber Membranes with Coagulation–Flocculation to Treat Colored Wastewater from a Dyestuff Manufacturer: A Pilot-Scale Study, Ind. Eng. Chem. Res., 54 (2015) 11159-11166. https://doi.org/10.1021/acs.iecr.5b03193

[29] Z. Thong, J. Gao, J.X.Z. Lim, K.-Y. Wang, T.-S. Chung, Fabrication of loose outer-selective nanofiltration (NF) polyethersulfone (PES) hollow fibers via single-step spinning process for dye removal, Sep. Purif. Technol., 192 (2018) 483-490. https://doi.org/10.1016/j.seppur.2017.10.031

[30] M. Cissé, F. Vaillant, D. Pallet, M. Dornier, Selecting ultrafiltration and nanofiltration membranes to concentrate anthocyanins from roselle extract (Hibiscus sabdariffa L.), Food Res. Int., 44 (2011) 2607-2614. https://doi.org/10.1016/j.foodres.2011.04.046

[31] J. Lin, C.Y. Tang, W. Ye, S.-P. Sun, S.H. Hamdan, A. Volodin, C.V. Haesendonck, A. Sotto, P. Luis, B. Van der Bruggen, Unraveling flux behavior of superhydrophilic loose nanofiltration membranes during textile wastewater treatment, J. Membr. Sci., 493 (2015) 690-702. https://doi.org/10.1016/j.memsci.2015.07.018

[32] Y. He, G.-M. Li, H. Wang, Z.-W. Jiang, J.-F. Zhao, H.-X. Su, Q.-Y. Huang, Experimental study on the rejection of salt and dye with cellulose acetate nanofiltration membrane, J. Taiwan Inst. Chem. Eng., 40 (2009) 289-295. https://doi.org/10.1016/j.jtice.2008.08.008

[33] T.-H. Kim, C. Park, S. Kim, Water recycling from desalination and purification process of reactive dye manufacturing industry by combined membrane filtration, J. Clean. Prod., 13 (2005) 779-786. https://doi.org/10.1016/j.jclepro.2004.02.044

[34] N. Tahri, G. Masmoudi, E. Ellouze, A. Jrad, P. Drogui, R. Ben Amar, Coupling microfiltration and nanofiltration processes for the treatment at source of dyeing-containing effluent, J. Clean. Prod., 33 (2012) 226-235. https://doi.org/10.1016/j.jclepro.2012.03.025

[35] I. Koyuncu, Reactive dye removal in dye/salt mixtures by nanofiltration membranes containing vinylsulphone dyes: effects of feed concentration and cross flow velocity, Desalination, 143 (2002) 243-253. https://doi.org/10.1016/S0011-9164(02)00263-1

[36] C. Tang, V. Chen, Nanofiltration of textile wastewater for water reuse, Desalination, 143 (2002) 11-20. https://doi.org/10.1016/S0011-9164(02)00216-3

[37] S. Guo, Y. Wan, X. Chen, J. Luo, Loose nanofiltration membrane custom-tailored for resource recovery, Chem. Eng. J., 409 (2021) 127376. https://doi.org/10.1016/j.cej.2020.127376

[38] X. Feng, D. Peng, J. Zhu, Y. Wang, Y. Zhang, Recent advances of loose nanofiltration membranes for dye/salt separation, Sep. Purif. Technol., (2021) 120228. https://doi.org/10.1016/j.seppur.2021.120228

[39] Y. Roy, D.M. Warsinger, J.H. Lienhard, Effect of temperature on ion transport in nanofiltration membranes: Diffusion, convection and electromigration, Desalination, 420 (2017) 241-257. https://doi.org/10.1016/j.desal.2017.07.020

[40] S. Gao, Y. Zhu, Y. Gong, Z. Wang, W. Fang, J. Jin, Ultrathin polyamide nanofiltration membrane fabricated on brush-painted single-walled carbon nanotube network support for ion sieving, ACS nano, 13 (2019) 5278-5290. https://doi.org/10.1021/acsnano.8b09761

[41] L. Venkataraman, J.E. Klare, C. Nuckolls, M.S. Hybertsen, M.L. Steigerwald, Dependence of single-molecule junction conductance on molecular conformation, Nature, 442 (2006) 904-907. https://doi.org/10.1038/nature05037

[42] S. Weigelt, C. Busse, L. Petersen, E. Rauls, B. Hammer, K.V. Gothelf, F. Besenbacher, T.R. Linderoth, Chiral switching by spontaneous conformational change in adsorbed organic molecules, Nature Mater., 5 (2006) 112-117. https://doi.org/10.1038/nmat1558

[43] J. Luo, Y. Wan, Effects of pH and salt on nanofiltration—a critical review, J. Membr. Sci., 438 (2013) 18-28. https://doi.org/10.1016/j.memsci.2013.03.029

[44] H. Zhang, Q. He, J. Luo, Y. Wan, S.B. Darling, Sharpening nanofiltration: Strategies for enhanced membrane selectivity, ACS Appl. Mater. Interfaces, 12 (2020) 39948-39966. https://doi.org/10.1021/acsami.0c11136

[45] D.L. Oatley, L. Llenas, R. Pérez, P.M. Williams, X. Martínez-Lladó, M. Rovira, Review of the dielectric properties of nanofiltration membranes and verification of the single oriented layer approximation, Adv. Colloid Interface Sci., 173 (2012) 1-11. https://doi.org/10.1016/j.cis.2012.02.001

[46] Y. Zhu, H. Zhu, G. Li, Z. Mai, Y. Gu, The effect of dielectric exclusion on the rejection performance of inhomogeneously charged polyamide nanofiltration membranes, J. Nanopart Res., 21 (2019) 1-13. https://doi.org/10.1007/s11051-019-4665-4

[47] J. Gao, T.-S. Chung, Influence of contaminants in glycerol/water mixtures during post-treatment on physicochemical properties and separation performance of air-dried membranes, J. Membr. Sci., 572 (2019) 223-229. https://doi.org/10.1016/j.memsci.2018.10.082

[48] P.W. Morgan, Condensation polymers: by interfacial and solution methods, Interscience Publishers, 1965.

[49] W. Lau, A. Ismail, N. Misdan, M. Kassim, A recent progress in thin film composite membrane: a review, Desalination, 287 (2012) 190-199. https://doi.org/10.1016/j.desal.2011.04.004

[50] P. Jin, S. Chergaoui, J. Zheng, A. Volodine, X. Zhang, Z. Liu, P. Luis, B. Van der Bruggen, Low-pressure highly permeable polyester loose nanofiltration membranes tailored by natural carbohydrates for effective dye/salt fractionation, J. Hazard. Mater., 421 (2022) 126716. https://doi.org/10.1016/j.jhazmat.2021.126716

[51] P. Jin, J. Zhu, S. Yuan, G. Zhang, A. Volodine, M. Tian, J. Wang, P. Luis, B. Van der Bruggen, Erythritol-based polyester loose nanofiltration membrane with fast water transport for efficient dye/salt separation, Chem. Eng. J., 406 (2021) 126796. https://doi.org/10.1016/j.cej.2020.126796

[52] J. Li, J.-L. Gong, G.-M. Zeng, B. Song, W.-C. Cao, S.-Y. Fang, S.-Q. Tang, Y. Guan, Z.-K. Tan, Z.-P. Chen, Thin-film composite polyester nanofiltration membrane with high flux and efficient dye/salts separation fabricated from precise molecular sieving structure of β-cyclodextrin, Sep. Purif. Technol., (2021) 119352. https://doi.org/10.1016/j.seppur.2021.119352

[53] L. Liu, L. Yu, B. Borjigin, Q. Liu, C. Zhao, D. Hou, Fabrication of thin-film composite nanofiltration membranes with improved performance using β-cyclodextrin as monomer for efficient separation of dye/salt mixtures, Appl. Surf. Sci., 539 (2021) 148284. https://doi.org/10.1016/j.apsusc.2020.148284

[54] J. Xue, J. Shen, R. Zhang, F. Wang, S. Liang, X. You, Q. Yu, Y. Hao, Y. Su, Z. Jiang, High-flux nanofiltration membranes prepared with β-cyclodextrin and graphene quantum dots, J. Membr. Sci., 612 (2020) 118465. https://doi.org/10.1016/j.memsci.2020.118465

[55] R. Xu, J. Wang, D. Chen, T. Liu, Z. Zheng, F. Yang, J. Chen, J. Kang, Y. Cao, M. Xiang, Preparation and performance of a charge-mosaic nanofiltration membrane with novel salt concentration sensitivity for the separation of salts and dyes, J. Membr. Sci., 595 (2020) 117472. https://doi.org/10.1016/j.memsci.2019.117472

[56] D.-D. Shao, L. Wang, X.-Y. Yan, X.-L. Cao, T. Shi, S.-P. Sun, Amine–carbon quantum dots (CQDs–NH2) tailored polymeric loose nanofiltration membrane for precise molecular separation, Chem. Eng. Res. Des., 171 (2021) 237-246. https://doi.org/10.1016/j.cherd.2021.04.031

[57] Y. Song, X. Bai, N. Zhang, Z. Lu, M. Zhu, Y. Wang, K. Jiang, Custom-tailoring tight nanocomposite membranes for advanced reclamation of hairwork dyeing effluent, J. Membr. Sci., 636 (2021) 119580. https://doi.org/10.1016/j.memsci.2021.119580

[58] Y. Song, Y. Wang, N. Zhang, X. Li, X. Bai, T. Li, Quaternized carbon-based nanoparticles embedded positively charged composite membranes towards efficient removal of cationic small-sized contaminants, J. Membr. Sci., 630 (2021) 119332. https://doi.org/10.1016/j.memsci.2021.119332

[59] Y. Song, Y. Sun, N. Zhang, C. Li, M. Hou, K. Chen, T. Li, Custom-tailoring loose nanocomposite membrane incorporated bipiperidine/graphene quantum dots for high-efficient dye/salt fractionation in hairwork dyeing effluent, Sep. Purif. Technol., 271 (2021) 118870. https://doi.org/10.1016/j.seppur.2021.118870

[60] Y. Li, R. Bi, Y. Su, Y. Li, C. Yang, X. You, J. Shen, J. Yuan, R. Zhang, Z. Jiang, Tuning the pore size of graphene quantum dots composite nanofiltration membranes by P-aminobenzoic acid for enhanced dye/salt separation, Sep. Purif. Technol., 263 (2021) 118372. https://doi.org/10.1016/j.seppur.2021.118372

[61] Q. Zhang, L. Fan, Z. Yang, R. Zhang, Y.-n. Liu, M. He, Y. Su, Z. Jiang, Loose nanofiltration membrane for dye/salt separation through interfacial polymerization with in-situ generated TiO2 nanoparticles, Appl. Surf. Sci., 410 (2017) 494-504. https://doi.org/10.1016/j.apsusc.2017.03.087

[62] Q. Li, Z. Liao, X. Fang, J. Xie, L. Ni, D. Wang, J. Qi, X. Sun, L. Wang, J. Li, Tannic acid assisted interfacial polymerization based loose thin-film composite NF membrane for dye/salt separation, Desalination, 479 (2020) 114343. https://doi.org/10.1016/j.desal.2020.114343

[63] Q. Guo, X. Wu, Y. Ji, Y. Hao, S. Liao, Z. Cui, J. Li, M. Younas, B. He, pH-responsive nanofiltration membrane containing chitosan for dye separation, J. Membr. Sci., 635 (2021) 119445. https://doi.org/10.1016/j.memsci.2021.119445

[64] S. Guo, H. Zhang, X. Chen, S. Feng, Y. Wan, J. Luo, Fabrication of Antiswelling Loose Nanofiltration Membranes via a "Selective-Etching-Induced Reinforcing" Strategy for Bioseparation, ACS Appl. Mater. Interfaces, 13 (2021) 19312-19323. https://doi.org/10.1021/acsami.1c02611

[65] Y. Kang, J. Jang, S. Kim, J. Lim, Y. Lee, I.S. Kim, PIP/TMC interfacial polymerization with electrospray: novel loose nanofiltration membrane for dye wastewater treatment, ACS Appl. Mater. Interfaces, 12 (2020) 36148-36158. https://doi.org/10.1021/acsami.0c09510

[66] Y. Liu, J. Zhu, J. Zheng, X. Gao, J. Wang, X. Wang, Y.F. Xie, X. Huang, B. Van der Bruggen, A Facile and Scalable Fabrication Procedure for Thin-Film Composite Membranes: Integration of Phase Inversion and Interfacial Polymerization, Environ. Sci. Technol., 54 (2020) 1946-1954. https://doi.org/10.1021/acs.est.9b06426

[67] D. Kang, H. Shao, G. Chen, X. Dong, S. Qin, Fabrication of highly permeable PVDF loose nanofiltration composite membranes for the effective separation of dye/salt mixtures, J. Membr. Sci., 621 (2021) 118951. https://doi.org/10.1016/j.memsci.2020.118951

[68] T. Wang, H. Wu, S. Zhao, W. Zhang, M. Tahir, Z. Wang, J. Wang, Interfacial polymerized and pore-variable covalent organic framework composite membrane for dye separation, Chem. Eng. J., 384 (2020) 123347. https://doi.org/10.1016/j.cej.2019.123347

[69] C. Mao, S. Zhao, P. He, Z. Wang, J. Wang, Covalent organic framework membranes with limited channels filling through in-situ grown polyaniline for efficient dye nanofiltration, Chem. Eng. J., 414 (2021) 128929. https://doi.org/10.1016/j.cej.2021.128929

[70] K. Tiwari, P. Sarkar, S. Modak, H. Singh, S.K. Pramanik, S. Karan, A. Das, Large Area Self-Assembled Ultrathin Polyimine Nanofilms Formed at the Liquid–Liquid Interface Used for Molecular Separation, Adv. Mater., 32 (2020) 1905621. https://doi.org/10.1002/adma.201905621

[71] C. Wang, Y. Chen, X. Hu, X. Feng, In-situ synthesis of PA/PVDF composite hollow fiber membranes with an outer selective structure for efficient fractionation of low-molecular-weight dyes-salts, Desalination, 503 (2021) 114957. https://doi.org/10.1016/j.desal.2021.114957

[72] M. Xu, X. Feng, X. Han, J. Zhu, J. Wang, B. Van der Bruggen, Y. Zhang, MOF laminates functionalized polyamide self-cleaning membrane for advanced loose nanofiltration, Sep. Purif. Technol., (2021) 119150. https://doi.org/10.1016/j.seppur.2021.119150

[73] T. Zhang, P. Li, S. Ding, X. Wang, High permeability composite nanofiltration membrane assisted by introducing TpPa covalent organic frameworks interlayer with nanorods for desalination and NaCl/dye separation, Sep. Purif. Technol., 270 (2021) 118802. https://doi.org/10.1016/j.seppur.2021.118802

[74] F. Aghili, A.A. Ghoreyshi, B. Van der Bruggen, A. Rahimpour, Introducing gel-based UiO-66-NH2 into polyamide matrix for preparation of new super hydrophilic membrane with superior performance in dyeing wastewater treatment, Journal of Environmental Chemical Engineering, 9 (2021) 105484. https://doi.org/10.1016/j.jece.2021.105484

[75] J. Ding, H. Wu, P. Wu, Preparation of highly permeable loose nanofiltration membranes using sulfonated polyethylenimine for effective dye/salt fractionation, Chem. Eng. J., 396 (2020) 125199. https://doi.org/10.1016/j.cej.2020.125199

[76] Y.F. Mi, N. Wang, Q. Qi, B. Yu, X.D. Peng, Z.H. Cao, A loose polyamide nanofiltration membrane prepared by polyether amine interfacial polymerization for dye desalination, Sep. Purif. Technol., 248 (2020) 117079. https://doi.org/10.1016/j.seppur.2020.117079

[77] S. Loeb, S. Sourirajan, Sea Water Demineralization by Means of an Osmotic Membrane, in: Saline Water Conversion—II, AMERICAN CHEMICAL SOCIETY, 1963, pp. 117-132. https://doi.org/10.1021/ba-1963-0038.ch009

[78] P. Jin, S. Yuan, G. Zhang, J. Zhu, J. Zheng, P. Luis, B. Van der Bruggen, Polyarylene thioether sulfone/sulfonated sulfone nanofiltration membrane with enhancement of rejection and permeability via molecular design☆, J. Membr. Sci., 608 (2020) 118241. https://doi.org/10.1016/j.memsci.2020.118241

[79] Y. Zhang, Q. Song, X. Liang, J. Wang, Y. Jiang, J. Liu, High-flux, high-selectivity loose nanofiltration membrane mixed with zwitterionic functionalized silica for dye/salt separation, Appl. Surf. Sci., 515 (2020) 146005. https://doi.org/10.1016/j.apsusc.2020.146005

[80] T. Tavangar, M. Karimi, M. Rezakazemi, K.R. Reddy, T.M. Aminabhavi, Textile waste, dyes/inorganic salts separation of cerium oxide-loaded loose nanofiltration polyethersulfone membranes, Chem. Eng. J., 385 (2020) 123787. https://doi.org/10.1016/j.cej.2019.123787

[81] H. Nawaz, M. Umar, A. Ullah, H. Razzaq, K.M. Zia, X. Liu, Polyvinylidene fluoride nanocomposite super hydrophilic membrane integrated with Polyaniline-Graphene oxide nano fillers for treatment of textile effluents, J. Hazard. Mater., 403 (2021) 123587. https://doi.org/10.1016/j.jhazmat.2020.123587

[82] N.S. Naik, M. Padaki, A.M. Isloor, K.K. Nagaraja, K.A. Vishnumurthy, Poly(ionic liquid)-Based charge and size selective loose nanofiltration membrane for molecular separation, Chem. Eng. J., 418 (2021) 129372. https://doi.org/10.1016/j.cej.2021.129372

[83] D.S. Dlamini, C. Matindi, G.D. Vilakati, J.M. Tesha, M.M. Motsa, J.M. Thwala, B.B. Mamba, E.M.V. Hoek, J. Li, Fine-tuning the architecture of loose nanofiltration membrane for improved water flux, dye rejection and dye/salt selective separation, J. Membr. Sci., 621 (2021) 118930.

[84] M. Hu, Z. Cui, S. Yang, J. Li, W. Shi, W. Zhang, C. Matindi, B. He, K. Fang, J. Li, Pregelation of sulfonated polysulfone and water for tailoring the morphology and properties of polyethersulfone ultrafiltration membranes for dye/salt selective separation, J. Membr. Sci., 618 (2021) 118746. https://doi.org/10.1016/j.memsci.2020.118746

[85] D. Ji, C. Xiao, S. An, J. Zhao, J. Hao, K. Chen, Preparation of high-flux PSF/GO loose nanofiltration hollow fiber membranes with dense-loose structure for treating textile wastewater, Chem. Eng. J., 363 (2019) 33-42. https://doi.org/10.1016/j.cej.2019.01.111

[86] G. Han, T.-S. Chung, M. Weber, C. Maletzko, Low-Pressure Nanofiltration Hollow Fiber Membranes for Effective Fractionation of Dyes and Inorganic Salts in Textile Wastewater, Environ. Sci. Technol., 52 (2018) 3676-3684. https://doi.org/10.1021/acs.est.7b06518

[87] Y. Liu, J. Wang, Y. Wang, H. Zhu, X. Xu, T. Liu, Y. Hu, High-flux robust PSf-b-PEG nanofiltration membrane for the precise separation of dyes and salts, Chem. Eng. J., 405 (2021) 127051. https://doi.org/10.1016/j.cej.2020.127051

[88] M. Hu, S. Yang, X. Liu, R. Tao, Z. Cui, C. Matindi, W. Shi, R. Chu, X. Ma, K. Fang, M. Titus, B.B. Mamba, J. Li, Selective separation of dye and salt by PES/SPSf tight ultrafiltration membrane: Roles of size sieving and charge effect, Sep. Purif. Technol., 266 (2021) 118587. https://doi.org/10.1016/j.seppur.2021.118587

[89] J. Jin, X. Du, J. Yu, S. Qin, M. He, K. Zhang, G. Chen, High performance nanofiltration membrane based on SMA-PEI cross-linked coating for dye/salt separation, J. Membr. Sci., 611 (2020) 118307. https://doi.org/10.1016/j.memsci.2020.118307

[90] C. Zhang, Y. Ou, W.X. Lei, L.S. Wan, J. Ji, Z.K. Xu, CuSO4/H2O2-induced rapid deposition of polydopamine coatings with high uniformity and enhanced stability, Angew. Chem. Int. Ed. Engl., 55 (2016) 3054-3057. https://doi.org/10.1002/anie.201510724

[91] J. Zhu, M.T. Tsehaye, J. Wang, A. Uliana, M. Tian, S. Yuan, J. Li, Y. Zhang, A. Volodin, B. Van der Bruggen, A rapid deposition of polydopamine coatings induced by iron (III) chloride/hydrogen peroxide for loose nanofiltration, J. Colloid Interface Sci., 523 (2018) 86-97. https://doi.org/10.1016/j.jcis.2018.03.072

[92] W. Ye, K. Ye, F. Lin, H. Liu, M. Jiang, J. Wang, R. Liu, J. Lin, Enhanced fractionation of dye/salt mixtures by tight ultrafiltration membranes via fast bio-inspired co-deposition for sustainable textile wastewater management, Chem. Eng. J., 379 (2020) 122321. https://doi.org/10.1016/j.cej.2019.122321

[93] J. Zhu, A. Uliana, J. Wang, S. Yuan, J. Li, M. Tian, K. Simoens, A. Volodin, J. Lin, K. Bernaerts, Elevated salt transport of antimicrobial loose nanofiltration membranes enabled by copper nanoparticles via fast bioinspired deposition, J. Mater. Chem. A, 4 (2016) 13211-13222. https://doi.org/10.1039/C6TA05661J

[94] X. Kang, Y. Cheng, Y. Wen, J. Qi, X. Li, Bio-inspired co-deposited preparation of GO composite loose nanofiltration membrane for dye contaminated wastewater sustainable treatment, J. Hazard. Mater., 400 (2020) 123121. https://doi.org/10.1016/j.jhazmat.2020.123121

[95] Q. Li, Z. Liao, X. Fang, D. Wang, J. Xie, X. Sun, L. Wang, J. Li, Tannic acid-polyethyleneimine crosslinked loose nanofiltration membrane for dye/salt mixture separation, J. Membr. Sci., 584 (2019) 324-332. https://doi.org/10.1016/j.memsci.2019.05.002

[96] Y. Cao, H. Zhang, S. Guo, J. Luo, Y. Wan, A robust dually charged membrane prepared via catechol-amine chemistry for highly efficient dye/salt separation, J. Membr. Sci., 629 (2021) 119287. https://doi.org/10.1016/j.memsci.2021.119287

[97] X.Q. Cheng, Z.X. Wang, Y. Zhang, Y. Zhang, J. Ma, L. Shao, Bio-inspired loose nanofiltration membranes with optimized separation performance for antibiotics removals, J. Membr. Sci., 554 (2018) 385-394. https://doi.org/10.1016/j.memsci.2018.03.005

[98] N. Zhang, B. Jiang, L. Zhang, Z. Huang, Y. Sun, Y. Zong, H. Zhang, Low-pressure electroneutral loose nanofiltration membranes with polyphenol-inspired coatings for effective dye/divalent salt separation, Chem. Eng. J., 359 (2019) 1442-1452. https://doi.org/10.1016/j.cej.2018.11.033

[99] J. Wang, R. He, X. Han, D. Jiao, J. Zhu, F. Lai, X. Liu, J. Liu, Y. Zhang, B. Van der Bruggen, High performance loose nanofiltration membranes obtained by a catechol-based route for efficient dye/salt separation, Chem. Eng. J., 375 (2019) 121982. https://doi.org/10.1016/j.cej.2019.121982

[100] M. Zhang, J. Gao, G. Liu, M. Zhang, H. Liu, L. Zhou, Y. Liu, X. Zheng, Y. Jiang, High-Throughput Zwitterion-Modified MoS2 Membranes: Preparation and Application in Dye Desalination, Langmuir, 37 (2021) 417-427. https://doi.org/10.1021/acs.langmuir.0c03068

[101] G. Li, B. Liu, L. Bai, Z. Shi, X. Tang, J. Wang, H. Liang, Y. Zhang, B. Van der Bruggen, Improving the performance of loose nanofiltration membranes by poly-dopamine/zwitterionic polymer coating with hydroxyl radical activation, Sep. Purif. Technol., 238 (2020) 116412. https://doi.org/10.1016/j.seppur.2019.116412

[102] Z. Zhao, M.A. Shehzad, B. Wu, X. Wang, A. Yasmin, Y. Zhu, X. Wang, Y. He, L. Ge, X. Li, T. Xu, Spray-deposited thin-film composite MOFs membranes for dyes removal, J. Membr. Sci., 635 (2021) 119475. https://doi.org/10.1016/j.memsci.2021.119475

[103] Y. Liang, S. Lin, Intercalation of zwitterionic surfactants dramatically enhances the performance of low-pressure nanofiltration membrane, J. Membr. Sci., 596 (2020) 117726. https://doi.org/10.1016/j.memsci.2019.117726

[104] M. Zhang, J. Gao, G. Liu, M. Zhang, H. Liu, L. Zhou, Y. Liu, X. Zheng, Y. Jiang, High-Throughput Zwitterion-Modified MoS2 Membranes: Preparation and Application in Dye Desalination, Langmuir, 37 (2020) 417-427. https://doi.org/10.1021/acs.langmuir.0c03068

[105] S. Zhao, Z. Wang, A loose nano-filtration membrane prepared by coating HPAN UF membrane with modified PEI for dye reuse and desalination, J. Membr. Sci., 524 (2017) 214-224. https://doi.org/10.1016/j.memsci.2016.11.035

[106] G. Li, W. Wang, Q. Fang, F. Liu, Covalent triazine frameworks membrane with highly ordered skeleton nanopores for robust and precise molecule/ion separation, J. Membr. Sci., 595 (2020) 117525. https://doi.org/10.1016/j.memsci.2019.117525

[107] D. Ji, C. Xiao, J. Zhao, K. Chen, F. Zhou, Y. Gao, T. Zhang, H. Ling, Green preparation of polyvinylidene fluoride loose nanofiltration hollow fiber membranes with multilayer structure for treating textile wastewater, Sci. Total Environ., 754 (2021) 141848. https://doi.org/10.1016/j.scitotenv.2020.141848

[108] J. Hu, M. Li, L. Wang, X. Zhang, Polymer brush-modified graphene oxide membrane with excellent structural stability for effective fractionation of textile wastewater, J. Membr. Sci., 618 (2021) 118698. https://doi.org/10.1016/j.memsci.2020.118698

[109] L. Dong, M. Li, S. Zhang, X. Si, Y. Bai, C. Zhang, NH2-Fe3O4-regulated graphene oxide membranes with well-defined laminar nanochannels for desalination of dye solutions, Desalination, 476 (2020) 114227. https://doi.org/10.1016/j.desal.2019.114227

[110] D. Xu, H. Liang, X. Zhu, L. Yang, X. Luo, Y. Guo, Y. Liu, L. Bai, G. Li, X. Tang, Metal-polyphenol dual crosslinked graphene oxide membrane for desalination of textile wastewater, Desalination, 487 (2020) 114503. https://doi.org/10.1016/j.desal.2020.114503

[111] J. Ma, Y. He, X. Tang, H. Yu, Y. Fan, T. He, S. Wang, Stable graphene oxide-halloysite composite membrane with enhanced permeability for efficient dye desalination, Sep. Purif. Technol., 266 (2021) 118067. https://doi.org/10.1016/j.seppur.2020.118067

[112] Y. Li, R. Dai, H. Zhou, X. Li, Z. Wang, Aramid Nanofiber Membranes Reinforced by MXene Nanosheets for Recovery of Dyes from Textile Wastewater, ACS Appl. Nano Mater., 4 (2021) 6328-6336. https://doi.org/10.1021/acsanm.1c01217

[113] Q. Long, S. Zhao, J. Chen, Z. Zhang, G. Qi, Z.-Q. Liu, Self-assembly enabled nano-intercalation for stable high-performance MXene membranes, J. Membr. Sci., 635 (2021) 119464. https://doi.org/10.1016/j.memsci.2021.119464

[114] J.-J. Han, Q.-Y. Zhang, M.-Y. Huang, Y. Chen, X. Yan, W.-Z. Lang, Two-dimensional WS2 membranes constructed on different substrates for efficient dye desalination, Desalination, 480 (2020) 114380. https://doi.org/10.1016/j.desal.2020.114380

[115] H. Zhao, G. Liu, M. Zhang, H. Liu, M. Zhang, L. Zhou, J. Gao, Y. Jiang, Bioinspired modification of molybdenum disulfide nanosheets to prepare a loose nanofiltration membrane for wastewater treatment, J. Water Process. Eng., 40 (2021) 101759. https://doi.org/10.1016/j.jwpe.2020.101759

[116] S. Zhou, X. Feng, J. Zhu, Q. Song, G. Yang, Y. Zhang, B. Van der Bruggen, Self-cleaning loose nanofiltration membranes enabled by photocatalytic Cu-triazolate MOFs for dye/salt separation, J. Membr. Sci., 623 (2021) 119058. https://doi.org/10.1016/j.memsci.2021.119058

[117] M. Xu, X. Feng, Z. Liu, X. Han, J. Zhu, J. Wang, B.V.d. Bruggen, Y. Zhang, MOF laminates functionalized polyamide self-cleaning membrane for advanced loose nanofiltration, Sep. Purif. Technol., 275 (2021) 119150. https://doi.org/10.1016/j.seppur.2021.119150

[118] Y. Li, R. Dai, H. Zhou, X. Li, Z. Wang, Aramid Nanofiber Membranes Reinforced by MXene Nanosheets for Recovery of Dyes from Textile Wastewater, ACS Appl. Mater. Interfaces, (2021). https://doi.org/10.1021/acsanm.1c01217

[119] N. Mehrabi, H. Lin, N. Aich, Deep eutectic solvent functionalized graphene oxide nanofiltration membranes with superior water permeance and dye desalination performance, Chem. Eng. J., 412 (2021) 128577. https://doi.org/10.1016/j.cej.2021.128577

[120] Y. Xu, G. Peng, J. Liao, J. Shen, C. Gao, Preparation of molecular selective GO/DTiO2-PDA-PEI composite nanofiltration membrane for highly pure dye separation, J. Membr. Sci., 601 (2020) 117727. https://doi.org/10.1016/j.memsci.2019.117727

[121] S. Liu, Z. Wang, P. Song, Free Radical Graft Copolymerization Strategy To Prepare Catechin-Modified Chitosan Loose Nanofiltration (NF) Membrane for Dye Desalination, ACS Sustainable Chem. Eng., 6 (2018) 4253-4263. https://doi.org/10.1021/acssuschemeng.7b04699

[122] Y.-S. Guo, Y.-L. Ji, B. Wu, N.-X. Wang, M.-J. Yin, Q.-F. An, C.-J. Gao, High-flux zwitterionic nanofiltration membrane constructed by in-situ introduction method for monovalent salt/antibiotics separation, J. Membr. Sci., 593 (2020) 117441. https://doi.org/10.1016/j.memsci.2019.117441

[123] C. Song, S. Tang, S. Yue, Z. Cui, X. Du, T. Jiang, B. He, J. Li, Design of microstructure for hollow fiber loose nanofiltration separation layer and its compactness-tailoring mechanism, J. Hazard. Mater., 421 (2022) 126800. https://doi.org/10.1016/j.jhazmat.2021.126800

[124] L. Bian, C. Shen, C. Song, S. Zhang, Z. Cui, F. Yan, B. He, J. Li, Compactness-tailored hollow fiber loose nanofiltration separation layers based on "chemical crosslinking and metal ion coordination" for selective dye separation, J. Membr. Sci., 620 (2021) 118948. https://doi.org/10.1016/j.memsci.2020.118948

[125] M. Halakarni, A. Mahto, K. Aruchamy, D. Mondal, S.K. Nataraj, Developing helical carbon functionalized chitosan-based loose nanofiltration membranes for selective separation and wastewater treatment, Chem. Eng. J., 417 (2021) 127911. https://doi.org/10.1016/j.cej.2020.127911

[126] S. Xiong, C. Han, A. Phommachanh, W. Li, S. Xu, Y. Wang, High-performance loose nanofiltration membrane prepared with assembly of covalently cross-linked polyethyleneimine-based polyelectrolytes for textile wastewater treatment, Sep. Purif. Technol., 274 (2021) 119105. https://doi.org/10.1016/j.seppur.2021.119105

[127] L. Huang, Z. Li, Y. Luo, N. Zhang, W. Qi, E. Jiang, J. Bao, X. Zhang, W. Zheng, B. An, G. He, Low-pressure loose GO composite membrane intercalated by CNT for effective dye/salt separation, Sep. Purif. Technol., 256 (2021) 117839. https://doi.org/10.1016/j.seppur.2020.117839

[128] Y.-J. Shen, Q.-R. Kong, L.-F. Fang, Z.-L. Qiu, B.-K. Zhu, Construction of covalently-bonded tannic acid/polyhedral oligomeric silsesquioxanes nanochannel layer for antibiotics/salt separation, J. Membr. Sci., 623 (2021) 119044. https://doi.org/10.1016/j.memsci.2020.119044

[129] L. Liu, S. Qu, Z. Yang, Y. Chen, Fractionation of Dye/NaCl Mixtures Using Loose Nanofiltration Membranes Based on the Incorporation of WS2 in Self-Assembled Layer-by-Layer Polymeric Electrolytes, Ind. Eng. Chem. Res., 59 (2020) 18160-18169. https://doi.org/10.1021/acs.iecr.0c03519

[130] S. Xu, D. Lu, P. Wang, Y. Zhao, Y. Sun, J. Qi, J. Ma, Polyphenol engineered membranes with dually charged sandwich structure for low-pressure molecular separation, J. Membr. Sci., 601 (2020) 117885. https://doi.org/10.1016/j.memsci.2020.117885

[131] Z. Gao, S. Liu, Z. Wang, S. Yu, Composite NF membranes with anti-bacterial activity prepared by electrostatic self-assembly for dye recycle, J. Taiwan Inst. Chem. Eng., 106 (2020) 34-50. https://doi.org/10.1016/j.jtice.2019.10.020

[132] X. You, K. Xiao, Q. Yu, H. Wu, J. Yuan, R. Zhang, Y. Ma, Y. Li, T. Huang, Z. Jiang, Fouling-resistant robust membranes via electrostatic complexation for water purification, Chem. Eng. J., 416 (2021) 129139. https://doi.org/10.1016/j.cej.2021.129139

[133] S. Zhao, H. Zhu, Z. Wang, P. Song, M. Ban, X. Song, A loose hybrid nanofiltration membrane fabricated via chelating-assisted in-situ growth of Co/Ni LDHs for dye wastewater treatment, Chem. Eng. J., 353 (2018) 460-471. https://doi.org/10.1016/j.cej.2018.07.081

[134] A. Metecan, A. Cihanoğlu, S. Alsoy Altinkaya, A positively charged loose nanofiltration membrane fabricated through complexing of alginate and polyethyleneimine with metal ions on the polyamideimide support for dye desalination, Chem. Eng. J., 416 (2021) 128946. https://doi.org/10.1016/j.cej.2021.128946

[135] C. Tian, S. Han, J. Zhu, S. Cao, J. Wang, R. Li, Y. Jin, Y. Zhang, B. Van der Bruggen, In situ growth of multifunctional porous organic polymer nanofilms with molecular sieving and catalytic abilities, Chem. Eng. J., 427 (2022) 130978. https://doi.org/10.1016/j.cej.2021.130978

[136] W.-H. Zhang, M.-J. Yin, Q. Zhao, C.-G. Jin, N. Wang, S. Ji, C.L. Ritt, M. Elimelech, Q.-F. An, Graphene oxide membranes with stable porous structure for ultrafast water transport, Nat. Nanotechnol., 16 (2021) 337-343. https://doi.org/10.1038/s41565-020-00833-9

[137] Z. Wang, Z. Si, D. Cai, G.L. Shufeng Li, P. Qin, Synthesis of stable COF-300 nanofiltration membrane via in-situ growth with ultrahigh flux for selective dye separation, J. Membr. Sci., 615 (2020) 118466. https://doi.org/10.1016/j.memsci.2020.118466

[138] Y. Zhang, K. Zhao, Z. Zhang, H. Xie, Z. Li, Z. Lin, C. Mo, W. Yang, X. Wang, J. Wei, Polypropylene non-woven supported calcium alginate hydrogel filtration membrane for efficient separation of dye/salt at low salt concentration, Desalination, 500 (2021) 114845. https://doi.org/10.1016/j.desal.2020.114845

[139] X.-l. Wang, W. Qin, L.-x. Wang, K.-y. Zhao, H.-c. Wang, H.-y. Liu, J.-f. Wei, Desalination of dye utilizing carboxylated TiO2/calcium alginate hydrogel nanofiltration membrane with high salt permeation, Sep. Purif. Technol., 253 (2020) 117475. https://doi.org/10.1016/j.seppur.2020.117475

[140] R.R. Choudhury, J.M. Gohil, S. Mohanty, S.K. Nayak, Antifouling, fouling release and antimicrobial materials for surface modification of reverse osmosis and nanofiltration membranes, J. Mater. Chem. A, 6 (2018) 313-333. https://doi.org/10.1039/C7TA08627J

[141] B. Van der Bruggen, L. Braeken, C. Vandecasteele, Evaluation of parameters describing flux decline in nanofiltration of aqueous solutions containing organic compounds, Desalination, 147 (2002) 281-288. https://doi.org/10.1016/S0011-9164(02)00553-2

[142] R. Zhang, Y. Liu, M. He, Y. Su, X. Zhao, M. Elimelech, Z. Jiang, Antifouling membranes for sustainable water purification: strategies and mechanisms, Chem. Soc. Rev., 45 (2016) 5888-5924. https://doi.org/10.1039/C5CS00579E

[143] X. Zhao, R. Zhang, Y. Liu, M. He, Y. Su, C. Gao, Z. Jiang, Antifouling membrane surface construction: Chemistry plays a critical role, J. Membr. Sci., 551 (2018) 145-171. https://doi.org/10.1016/j.memsci.2018.01.039

[144] J. Zhu, J. Wang, A.A. Uliana, M. Tian, Y. Zhang, Y. Zhang, A. Volodin, K. Simoens, S. Yuan, J. Li, Mussel-inspired architecture of high-flux loose nanofiltration membrane functionalized with antibacterial reduced graphene oxide–copper nanocomposites, ACS Appl. Mater. Interfaces, 9 (2017) 28990-29001. https://doi.org/10.1021/acsami.7b05930

[145] S. Zhou, J. Gao, J. Zhu, D. Peng, Y. Zhang, Y. Zhang, Self-cleaning, antibacterial mixed matrix membranes enabled by photocatalyst Ti-MOFs for efficient dye removal, J. Membr. Sci., 610 (2020) 118219. https://doi.org/10.1016/j.memsci.2020.118219

[146] H. Zhang, Y. Wan, J. Luo, S.B. Darling, Drawing on Membrane Photocatalysis for Fouling Mitigation, ACS Appl. Mater. Interfaces, 13 (2021) 14844-14865. https://doi.org/10.1021/acsami.1c01131

[147] W. Zhang, L. Ding, J. Luo, M.Y. Jaffrin, B. Tang, Membrane fouling in photocatalytic membrane reactors (PMRs) for water and wastewater treatment: A critical review, Chem. Eng. J., 302 (2016) 446-458. https://doi.org/10.1016/j.cej.2016.05.071

[148] X. Meng, J. Ren, J. Chen, J. Song, H. Zheng, L. Wang, D. Huang, Ag3PO4 composite nanofiltration membrane and its visible-light photocatalytic properties, J. Membr. Sci., 631 (2021) 119334. https://doi.org/10.1016/j.memsci.2021.119334

[149] Y. Wei, Y. Zhu, Y. Jiang, Photocatalytic self-cleaning carbon nitride nanotube intercalated reduced graphene oxide membranes for enhanced water purification, Chem. Eng. J., 356 (2019) 915-925. https://doi.org/10.1016/j.cej.2018.09.108